Journal of Structural Geology 30 (2008) 1429–1447

Contents lists available at ScienceDirect

Journal of Structural Geology

journal homepage: www.elsevier.com/locate/jsg

The form, distribution and anisotropy of magnetic susceptibility of Jurassic dykes in H.U. Sverdrupfjella, Dronning Maud Land, Antarctica. Implications for dyke swarm emplacement

Michael L. Curtis [a,*], Teal R. Riley [a], William H. Owens [b,†], Philip T. Leat [a], Robert A. Duncan [c]

[a] British Antarctic Survey, NERC, High Cross, Madingley Road, Cambridge CB3 0ET, UK
[b] School of Geography, Earth & Environmental Sciences, University of Birmingham, Edgbaston, Birmingham, B15 2TT, UK
[c] College of Oceanic and Atmospheric Sciences, Oregon State University, Corvallis, OR 97331-5503, USA

ARTICLE INFO

Article history:
Received 21 September 2007
Received in revised form 4 July 2008
Accepted 23 August 2008
Available online 10 September 2008

Keywords:
Radial dykes
Magma flow
Gondwana break-up
Karoo

ABSTRACT

The Mesozoic dyke swarms of Western Dronning Maud Land, Antarctica, form a minor intrusive component of the Karoo large igneous province. Five-hundred and sixty one dykes were recorded intruding Neoproterozoic gneisses and Middle Jurassic syenite plutons. $^{40}Ar/^{39}Ar$ geochronology data reveal two temporally distinct components: the 178–175 Ma, alkaline, Straumsvola dyke swarm that predominantly intrudes a nepheline syenite pluton; and the 206–204 Ma, tholeiitic, Jutulrøra dyke swarm found throughout the study area. The Straumsvola swarm exhibits highly variably dyke trends that display a restricted opening direction, interpreted to be the result of high magma pressure equal to the maximum principal stress. The Jutulrøra swarm displays a fan of dyke trends, with dyke thickness and spacing increasing away from the inferred point of fan convergence. Anisotropy of magnetic susceptibility measurements reveal vertical magma transport within both dyke swarms in the Straumsvola area, with the southern/outer exposures of the Jutulrøra swarm exhibiting lateral magma transport. Although associated with a long-lived, local igneous centre comparison of palaeostress estimates for the Straumsvola dyke swarm and contemporaneous dykes in Ahlmannryggen and Vestfjella, indicates the presence of a regional scale radial stress system in western Dronning Maud Land between 178–175 Ma, supporting a mantle plume origin for the Karoo large igneous province.

1. Introduction

The Early to Middle Jurassic Karoo and Ferrar large igneous provinces of southern Africa and Antarctica cover 6×10^6 km^2 (Le Gall et al., 2002) and together represent one of the largest continental magmatic events in Phanerozoic Earth history. The Ferrar large igneous province (LIP) is exposed along the length of the Transantarctic Mountains where it is dominated by massive, laterally extensive dolerite sills (Elliot et al., 1999), a mafic layered intrusion at Dufek Massif (Ford and Himmelberg, 1991), and a capping volcanic succession, the Kirkpatrick basalts (Kyle, 1980). The Karoo LIP of southern Africa and its Antarctic component in western Dronning Maud Land, East Antarctica, expose predominantly low-Ti tholeiitic flood basalts (Harris et al., 1990; Marsh et al., 1997) that were erupted within a 3–4 Myr period at c. 182 Ma (Riley and Knight, 2001), although magmatism in both regions occurred over a longer period (Riley et al., 2005; Jourdan et al., 2004). In addition to the voluminous flood basalts, widespread sill complexes in southern Africa are accompanied by four giant dyke swarms; the N110° Okavango dyke swarm (ODS), the N70°E Sabi–Limpopo dyke swarm (SLDS), the north–south trending Lebombo dyke swarm (LDS), and the N20–40°W trending Olifants River dyke swarm (ORDS) (Le Gall et al., 2002). The dykes within the ODS and SLDS have average widths of 18 m and 35 m, respectively (Le Gall et al., 2002), and were predominantly emplaced at c.178 Ma after peak Karoo magmatism at c. 182 Ma (Elburg and Goldberg, 2000; Le Gall et al., 2002; Jourdan et al., 2004). These dyke swarms converge on the Mwenezi region of southern Zimbabwe to form an apparent giant radiating dyke swarm, which has been interpreted to indicate the presence of a rift triple junction above the site of a former mantle plume (Burke and Dewey, 1972; White and McKenzie, 1989), although this interpretation has been questioned (Le Gall et al., 2002; Jourdan et al., 2004).

In western Dronning Maud Land (Fig. 1), Karoo magmatic activity appears to have been less intense. Flood basalt lava sequences crop out at Vestfjella, Heimefrontfjella, and Kirwanveggen, although they are thinner (<1 km thickness; Luttinen and

* Corresponding author. Tel.: +44 1223 221429
E-mail address: mlcu@bas.ac.uk (M.L. Curtis).
† Deceased.

0191-8141/$ – see front matter
doi:10.1016/j.jsg.2008.08.004

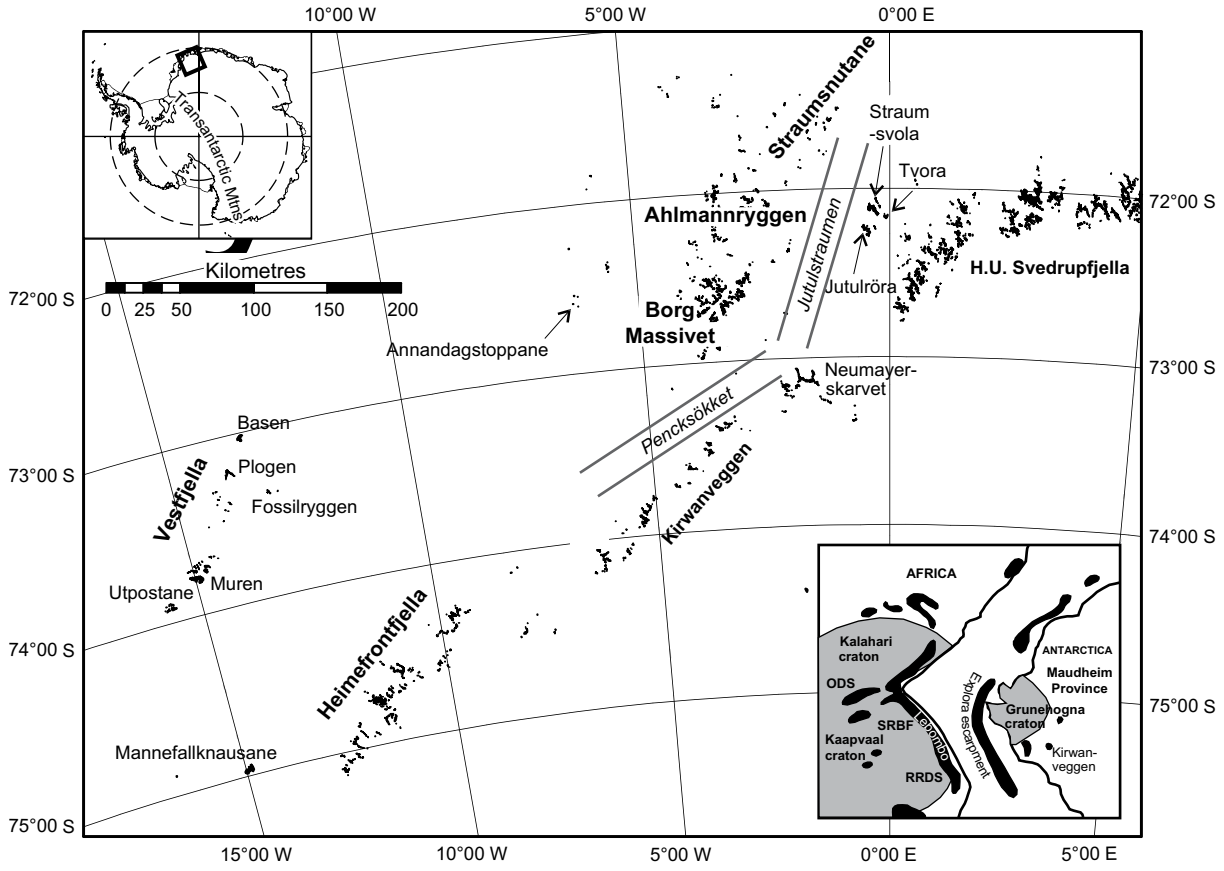

Fig. 1. Location map of rock outcrops in western Dronning Maud Land (Antarctica) from Vestfjella to H.U. Svedrupfjella, including the location of the Jutustraumen and Pencksökket subglacial troughs. The inset is a pre-break-up Gondwana reconstruction of Africa and Antarctica showing the extent of the Kaapvaal-Grunehogna craton and the outcrop of Early–Middle Jurassic Karoo igneous rocks (after Luttinen and Furnes, 2000). ODS, Okavango dyke swarm; SRBF, Sabi River Basalt Formation; RRDS, Rooi Rand dyke swarm. After Riley et al. (2005).

Furnes, 2000) than their African equivalents. Although there are no flood basalts within the Jutulstraumen area, several suites of Early to Middle Jurassic mafic dykes occur in the Ahlmannryggen (Harris et al., 1991; Riley et al., 2005) and H.U. Sverdrupfjella regions (Grantham, 1996). However, in contrast to their contemporaneous African dyke swarms, these dykes are on a much smaller scale with widths typically <2 m (Riley et al., 2005).

In this paper, we present new geochronological, structural, and anisotropy of magnetic susceptibility (AMS) data for mafic dykes from H.U. Sverdrupfjella. We propose that these dykes were locally sourced from a long-lived igneous centre but were emplaced in a regional radial stress field associated a mantle plume.

2. Background geology

The geology of western Dronning Maud is summarised in Fig. 1, and can be subdivided into two distinct geological provinces. The Grunehogna province, which occupies the Ahlmannryggen, Borgmassivet, and Straumsnutane areas, together with outlying nunataks to the west, is characterised by weakly metamorphosed and deformed sedimentary and volcanogenic rocks of the Ritscherfjella Supergroup that have been extensively intruded by large-scale tholeiitic sills and dykes of the Borgmassivet Intrusions (Wolmarans and Kent, 1982) emplaced between 900 and 1100 Ma (Wolmarans and Kent, 1982; Moyes et al., 1995). The basement to the Ritscherfjella Supergroup is considered to be Achaean age granitoids, similar to those exposed at Annandagstoppan. To the south and east of the Grunehogna province lie the Kirwanveggen and H.U. Sverdrupfjella regions that form part of the Mesoproterozoic Maud province, an extension of the Namaqua-Natal metamorphic province of southern Africa (Jacobs et al., 1993), which is formed of amphibolite to granulite facies gneisses of the Jutulrøra Formation (Svedrupfjella Group) (Groenewald et al., 1995).

The crustal boundary between these two geological provinces lies beneath the Pencksökket and Jutulstraumen ice streams and is interpreted as being reactivated by a Mesozoic continental rift that was either amagmatic along its axis or contains a thick sedimentary succession (Ferraccioli et al., 2005a,b).

Two alkaline plutons occur within the eastern flank of the Jutulstraumen rift centred on Straumsvola and Tvora nunataks (Fig. 2). Geochronology of the intrusions has yielded a range of ages, but the best estimates for the Straumsvola pluton are in the range, 174–180 Ma, with an age of >178 Ma preferred based on cross-cutting dolerite dykes. The Tvora pluton has yielded an $^{40}Ar/^{39}Ar$ (hornblende) age of 183 ± 2 Ma, although Grantham et al. (1988) regarded this as a reset age and favoured a 207 ± 5 Ma (Rb–Sr) age.

The Straumsvola nepheline syenite complex is approximately 7 km in diameter and is composed of a relatively structureless outer zone of coarsely crystalline, leucocratic nepheline syenite, and an internal layered zone (Harris and Grantham, 1993). The smaller Tvora quartz syenite pluton is approximately 3 km in diameter and forms the bulk of the Tvora nunatak group. Both plutons intrude gneisses of the Jutulrøra Formation and are associated with localised positive magnetic anomalies (Ferraccioli et al., 2005a) and gravity highs, suggesting that significant mafic bodies underlie them (Ferraccioli et al., 2005b).

Mafic dykes intrude both flanks of the Jutulstraumen rift. In the western or Ahlmannryggen flank mafic dykes form two structurally

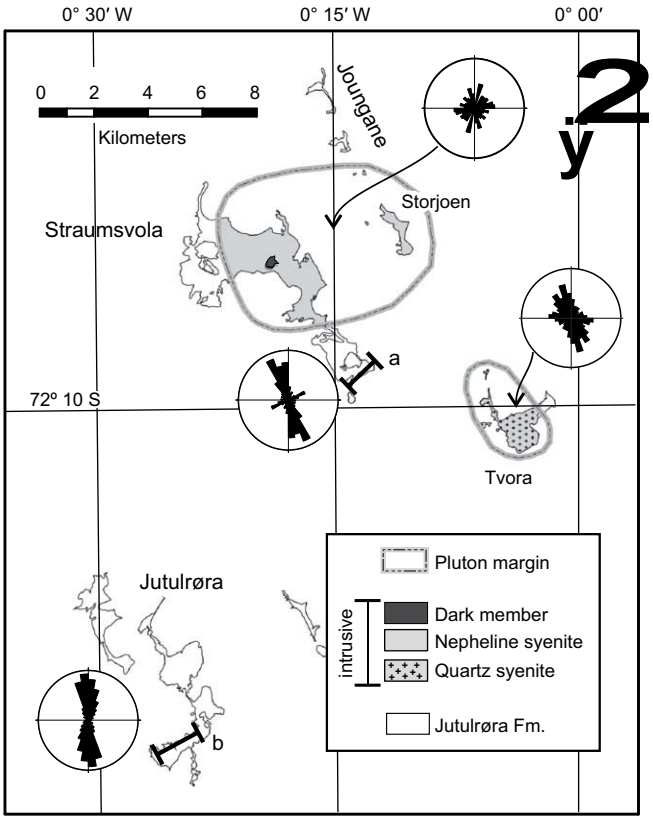

Fig. 2. Geological map of northwestern H.U. Svedrupfjella displaying the location of Early–Middle Jurassic syenite plutons at Straumsvola and Tvora. The location of two structural traverses, labelled (a), (b), are shown, as are rose diagrams for local dyke orientation.

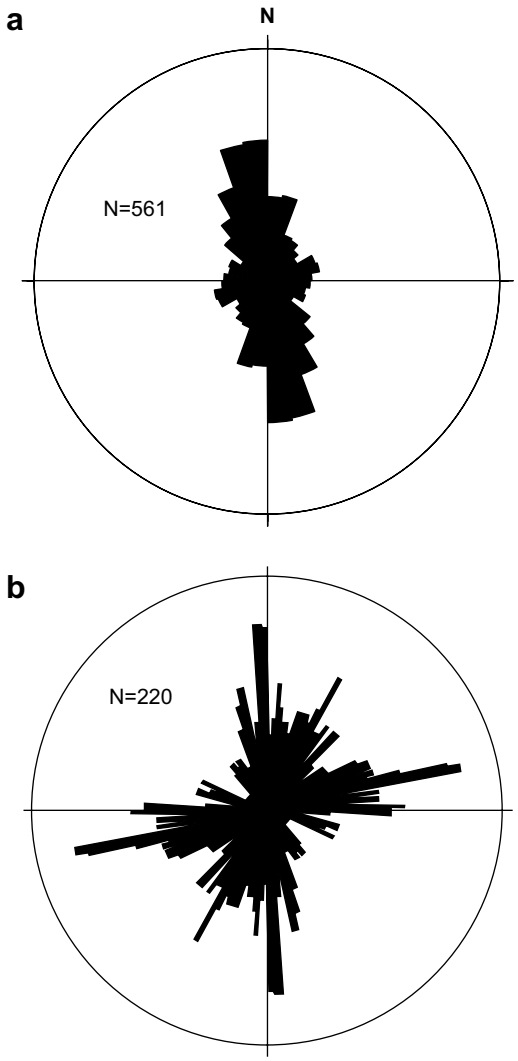

Fig. 3. (a) Rose diagram of dyke strike for all dykes recorded in the H.U. Svedrupfjella dyke swarm at Straumsvola, Tvora and Jutulrøra nanataks. (b) Rose diagram showing all joints measured in H.U. Sverdrupfjella by Hjelle (1972).

and geochemically distinct dyke suites emplaced at 190 and 178 Ma, trending sub-parallel to the local boundaries of the Grunehogna craton (Riley et al., 2005). The presence of ferropicrite and picrite dykes, together with other geochemical and isotopic evidence, indicates that many of the Ahlmannryggen dykes were sourced at great depth and anomalously high temperature, indicative of mantle plume derivation (Riley et al., 2005).

In H.U. Sverdrupfjella, along the eastern flank of the Jutustraumen rift, numerous mafic dykes intrude Jutulrøra Formation gneisses, as well as the syenite plutons at Straumsvola and Tvora (Harris and Grantham, 1993; Grantham, 1996). The emplacement of these dykes and their regional significance for Karoo age magmatism and tectonics is the subject of this study.

3. Dyke swarms of H.U. Sverdrupfjella

A total of 561 dykes were recorded within the nunatak groups of Straumsvola, Tvora and Jutulrøra. As previously highlighted by Grantham (1996), the dyke swarm has a pronounced NNW–SSE trend with a subcomponent of ENE–WSW trending dykes, with the main dyke trends intruded parallel to measured joints (Fig. 3). The majority (81%) of the dykes are doleritic, typically fine to medium grained and feldspar-phyric, commonly displaying glassy chilled margins. Rare phenocrysts of augite and unaltered olivine can also be identified in hand specimen. Unpublished geochemical analysis reveals the dolerite dykes have two distinct compositions, with dykes intruding the syenite plutons being alkaline basanites to tephrites, while those intruding the country rock gneisses at Straumsvola and Jutulrøra nunataks are overwhelmingly low-Ti and low-Zr tholeiites. A third significant set of dykes is phonolitic or trachytic in composition and represents the final intrusive phase of the dyke suite, cross-cutting dolerite dykes and syenitic pegmatites and accounts for 8% of the dyke swarm.

The following sections detail the geochronological, structural and anisotropy of magnetic susceptibility characteristics of the H.U. Sverdrupfjella dyke swarms.

4. Geochronology

There is only limited pre-existing geochronology for the H.U. Sverdrupfjella dyke swarms. Grantham et al. (1988) report $^{40}Ar/^{39}Ar$ (plagioclase) ages in the range 172–199 Ma, but there was no geochemical or structural control reported on the analysed samples.

For this study eight samples of dykes (Z.1902.7, Z.1904.3, Z.1911.4, Z.1911.7, Z.1919.5, Z.1926.6, Z.1928.3, Z.1933.3) were selected for $^{40}Ar/^{39}Ar$ geochronology, providing the best possible spread based on geographical and structural relationships.

4.1. Analytical methods

Samples were 5 mm diameter whole rock cores packaged in evacuated quartz vials, and were irradiated in the Oregon State

University TRIGA Reactor for 6 h at 1 MW power. The neutron flux was measured using standard FCT-3 biotite, 28.03 Ma (Renne et al., 1998). Reactor temperatures can reach up to 270 °C. Additionally, samples were baked at 195 °C for 48 hours during extraction line pump-down to $\sim 10^{-9}$ torr.

Depending on sample composition, the incremental heating experiment started in the range 400–600 °C and was typically complete by 1400 °C, using a Heine low-blank resistance furnace with a Ta–Nb-crucible and Mo-liner. Each heating step was 20 min duration with an additional 5 min cooling and continued removal of active gases with St101 Zr-Al and St172 Zr-V-Fe getters.

A MAP 215-50 rare gas mass spectrometer source at 3000 V, and equipped with a Johnston MM1-1SG electron multiplier at 2050 V was used for analysis. During the 15 min analysis time per mass peak height, data were collected for 10 cycles of masses 35–40 for baselines and peak-tops. Data were reduced and age calculations were completed using ArArCALC v2.2 software for $^{40}Ar/^{39}Ar$ geochronology (Koppers, 2002).

4.2. Results

The $^{40}Ar/^{39}Ar$ results are presented in Fig. 4(a–h). Data from seven of the eight samples presented satisfy the key criteria for reliable age data, (1) multiple (three or more) concordant step ages comprising >50% of the total gas released, (2) concordant plateau and isochron ages, (3) low MSWDs (<3) for plateau and isochron ages.

Whole rock sample Z.1904.3 yielded an excellent mid-high temperature, 5-step plateau (174.7 ± 1.8 Ma; Fig. 4a) comprising 70% of total gas released and is the preferred age. An additional two steps almost fall on the same plateau. The isochron is concordant at 174.8 ± 2.0 Ma.

Whole rock sample Z.1911.4 also yielded an excellent mid-temperature, three-step plateau (175.4 ± 2.0 Ma; Fig. 4b) comprising 62% of gas released. The U-shaped pattern of this age spectrum is indicative of excess argon in the low- and high-temperature steps. However, the broad mid-temperature plateau is interpreted to be a good estimate of the crystallization age. The isochron age of 180.4 ± 23.0 Ma is statistically poor.

Whole rock sample Z.1911.7 (phonolite) provided a good low- to high-temperature, 10-step plateau (170.9 ± 1.7 Ma; Fig. 4c) comprising 95% of total gas released and is the preferred age. The isochron is concordant at 169.5 ± 1.8 Ma, although the $^{40}Ar/^{39}Ar$ intercept on the isochron is higher than the atmospheric value.

Whole rock sample Z.1919.5 provided a good mid- to high-temperature, five-step plateau (178.5 ± 1.5 Ma; Fig. 4d) comprising almost 70% of the total gas released and is the preferred age. The isochron is concordant at 177.3 ± 3.4 Ma.

Whole rock sample Z.1926.6 provided a good high-temperature, five-step plateau (176.3 ± 1.6 Ma; Fig. 4e) comprising 56% of total gas released and is the preferred age. The isochron is concordant at 175.1 ± 7.7 Ma. There is slight ^{40}Ar loss (first step) and ^{39}Ar recoil at high temperature.

Whole rock sample Z.1933.3 provided a good mid-temperature, four-step plateau (203.8 ± 2.8 Ma; Fig. 4f) comprising 78% of total gas released and is the preferred age. Unlike the other samples of this study, the isochron is almost concordant, yielding an age of 196.8 ± 4.5 Ma.

Whole rock sample Z.1928.3 provided a good mid-temperature, four-step plateau (206.1 ± 2.6 Ma; Fig. 4 g) comprising 68% of total gas released and is the preferred age. The isochron is also concordant at 203.2 ± 3.4 Ma. There is slight ^{40}Ar loss at the third step.

Whole rock sample Z.1902.7 failed to satisfy the key criteria for a reliable age data, producing a seven step weighed plateau (212.8 ± 8.7 Ma, Fig. 4h). We interpret this sample to have been affected by excess argon.

4.3. Summary of geochronology

Our new geochronological data reveals the presence of three temporally distinct dyke emplacement events that are also geographically and geochemically distinct.

Two samples from low-Ti, low-Zr tholeiite dykes record a dyke emplacement event between 206 and 204 Ma. At Jutulrøra nunataks two dykes intruding the Jutulrøra Formation orthogneisses yield whole rock ages of 206.1 ± 2.6 (Z.1928.3) and 203.8 ± 2.8 Ma (Z.1933.3). A third tholeiite dyke sample (Z.1902.7) intruding Jutulrøra Formation gneisses at Straumsvola has been affected by excess argon. This dyke emplacement event predated the emplacement of the Straumsvola nepheline syenite.

Another generation of dyke emplacement is recorded in the interval 174.8–178.5 Ma by four samples of basanite/tephrite composition dykes, two of them (Z.1911.4, Z.1919.5) intrude the Straumsvola syenite pluton, which has been dated at 178–180 Ma (Grantham et al., 1998). A third sample (Z.1904.3) intrudes the country rock gneiss adjacent to the Straumsvola syenite, whilst the fourth sample is from a dyke intruding the neighbouring Tvora quartz syenite pluton.

Sample Z.1911.7 is a late stage phonolite dyke, also from the Straumsvola pluton and has a whole rock age of 170.9 ± 1.7 Ma, which is significantly younger than the mafic dyke suite, which it crosscuts. This date provides an upper age constraint on the duration of magmatism within the Straumsvola intrusive suite.

Although our results broadly support those of Grantham et al. (1998) who suggested that magmatism within the region was long-lived (170–206 Ma), our data reveals that the mafic component of the dyke swarm is actually composed of two temporally distinct dyke emplacement events. In recognition of this, we will refer to the 175–178 Ma alkaline dykes that intrude the Straumsvola and Tvora syenite plutons as the Straumsvola dyke swarm, and the 206–204 Ma tholeiite dykes that predominate within the country rock gneisses as the Jutulrøra dyke swarm.

5. Variability within the Straumsvola and Jutulrøra dyke swarms

5.1. Dyke orientation and composition

Straumsvola dyke swarm: at Straumsvola and the neighbouring nunataks of Joungane and Storjoen, 172 dykes were recorded cutting the nepheline syenite. Virtually all the dykes postdate solidification of the pluton, although rare syn-plutonic mafic dykes were observed. Dykes strike in virtually every direction, although there is a biased toward NE–SW orientations (Fig. 5a), while dyke dip also varies greatly with 46% inclined at <60°. The majority of dykes vary in width between 0.06 and 8.5 m, with three exceptions ranging between 11 and 21 m. Lithologically, the dyke population is dominated by dolerite dykes (65%), with a significant percentage of more felsic (20%) or phonolitic (13%) dykes (Fig. 6a). There is little or no relationship between dyke orientation and dyke lithology.

A complete traverse of Tvora recorded 74 dykes, 29 intruding the gneissic country rocks and 45 within the quartz syenite pluton. The Tvora dyke swarm has a pronounced NNW–SSE trend with a subordinate E–W trending component, and varies between 0.04 and 7.5 m in thickness (Fig. 5b). In general, the dyke population is steeply inclined with 84% dipping at >60° and there are no significant differences between the geometries of the dyke populations within or outside the quartz syenite pluton. The Tvora dykes are predominantly doleritic (76%), with a relatively high percentage of lamprophyre dykes (13%). Although these various dyke lithologies are fairly evenly represented within the main trends of the Tvora dyke population, the greatest lithological

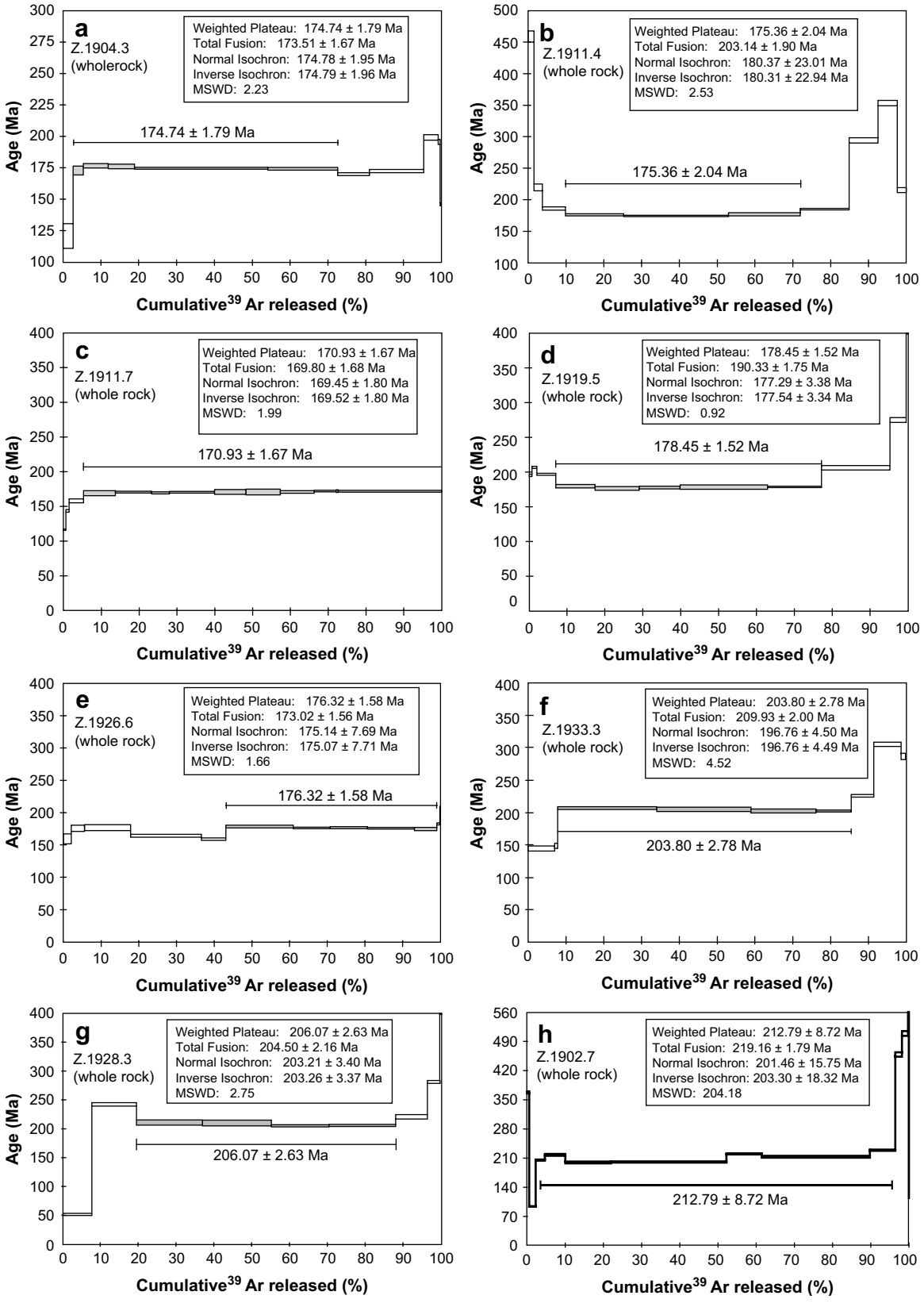

Fig. 4. ^{39}Ar release spectra for samples Z.1902.7, Z.1904.3, Z.1911.4, Z.1911.7, Z.1919.5, Z.1926.6, Z.1933.3 and Z.1928.3. Seven samples generated a plateau that satisfied the key criteria for reliable age data, (1) multiple (three or more) concordant step ages comprising >50% of the total gas released, (2) concordant plateau and isochron ages, (3) low MSWDs (<3) for plateau and isochron ages.

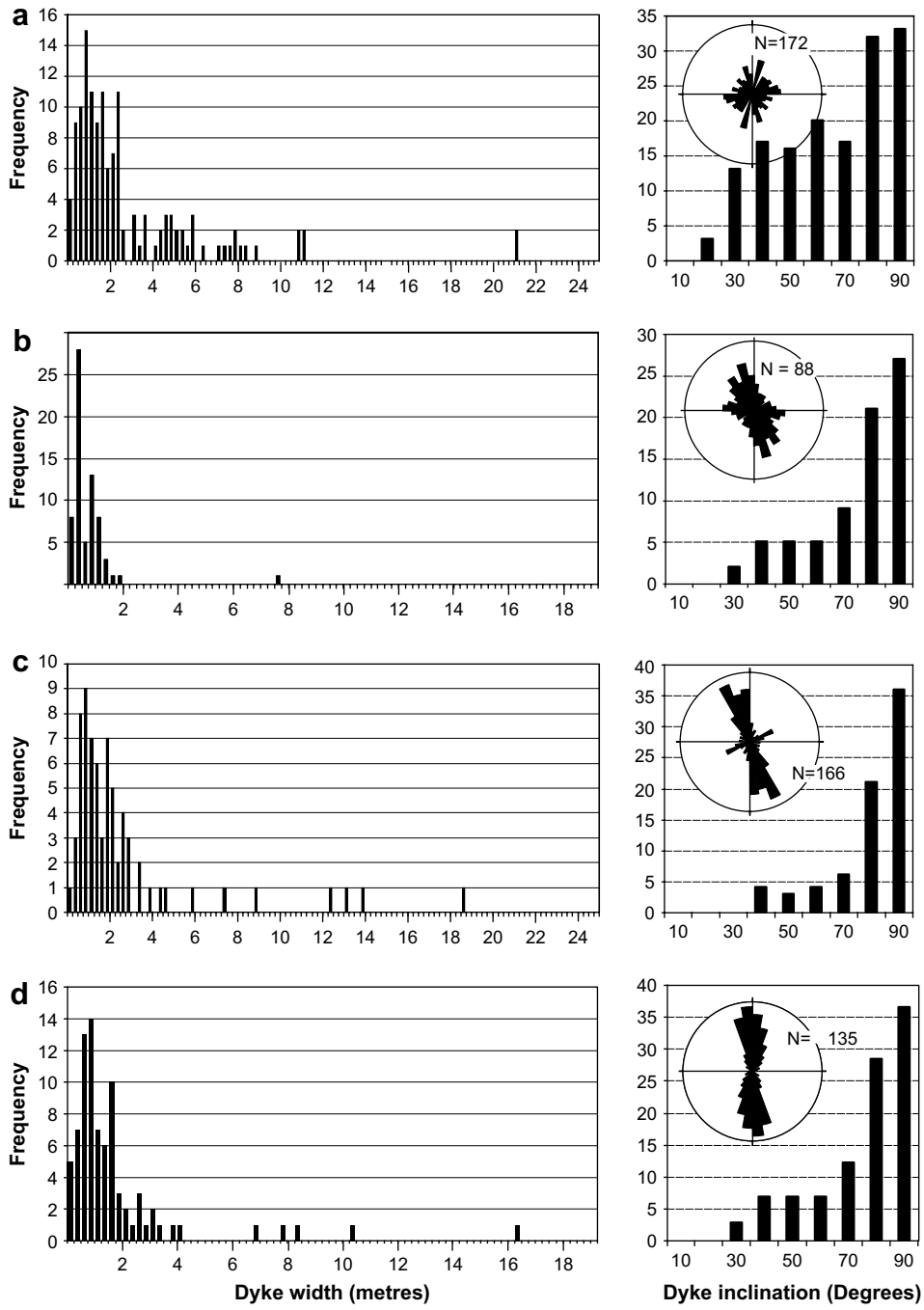

Fig. 5. Geometry of dykes intruding (a) the nepheline syenite pluton at Straumsvola, (b) Tvora quartz syenite and immediate country rocks, (c) the country rock surrounding the Straumsvola pluton, (d) Jutulrøra nunataks. The dyke population in each sub-area is represented by frequency vs. dyke width, frequency vs. dyke inclination, and frequency vs. orientation (rose) diagrams.

diversity is found in dykes trending between E–W and NW–SE (Fig. 5b). Where cross-cutting relationships exist lamprophyre and phonolite dykes are generally the youngest.

Jutulrøra dyke swarm: 166 dykes were recorded intruding the country rock gneisses adjacent to the Straumsvola nepheline syenite. In contrast to the younger alkaline dykes intruding the pluton, the tholeiitic dykes display a pronounced NNW–SSE trend with a subordinate NE–SW population, and are generally more steeply inclined with 85% possessing an inclination $>60^{\circ}$ (Fig. 5c). Dyke widths vary from 0.06 to 19.2 m. NNW–SSE trending dykes are overwhelmingly doleritic (91%), while NE–SW to E–W trending dykes display a varied lithological range including pegmatite, lamprophyre and phonolite (Fig. 6c) which are probably part of the Straumsvola swarm.

Approximately 15 km southeast of Straumsvola, Jutulrøra nunataks exposes at least 135 predominantly tholeiitic dykes intruding Jutulrøra Formation gneisses. The dyke swarm is N–S trending and steeply inclined, with 85% of dykes dipping at $>60^{\circ}$ (Fig. 5d), and dyke widths varying from 0.04 to 22 m. The dykes are almost exclusively doleritic (97%) (Fig. 6d), typically feldspar-pyroxene phyric, and display chilled margins. The remaining dykes identified were two lamprophyre dykes.

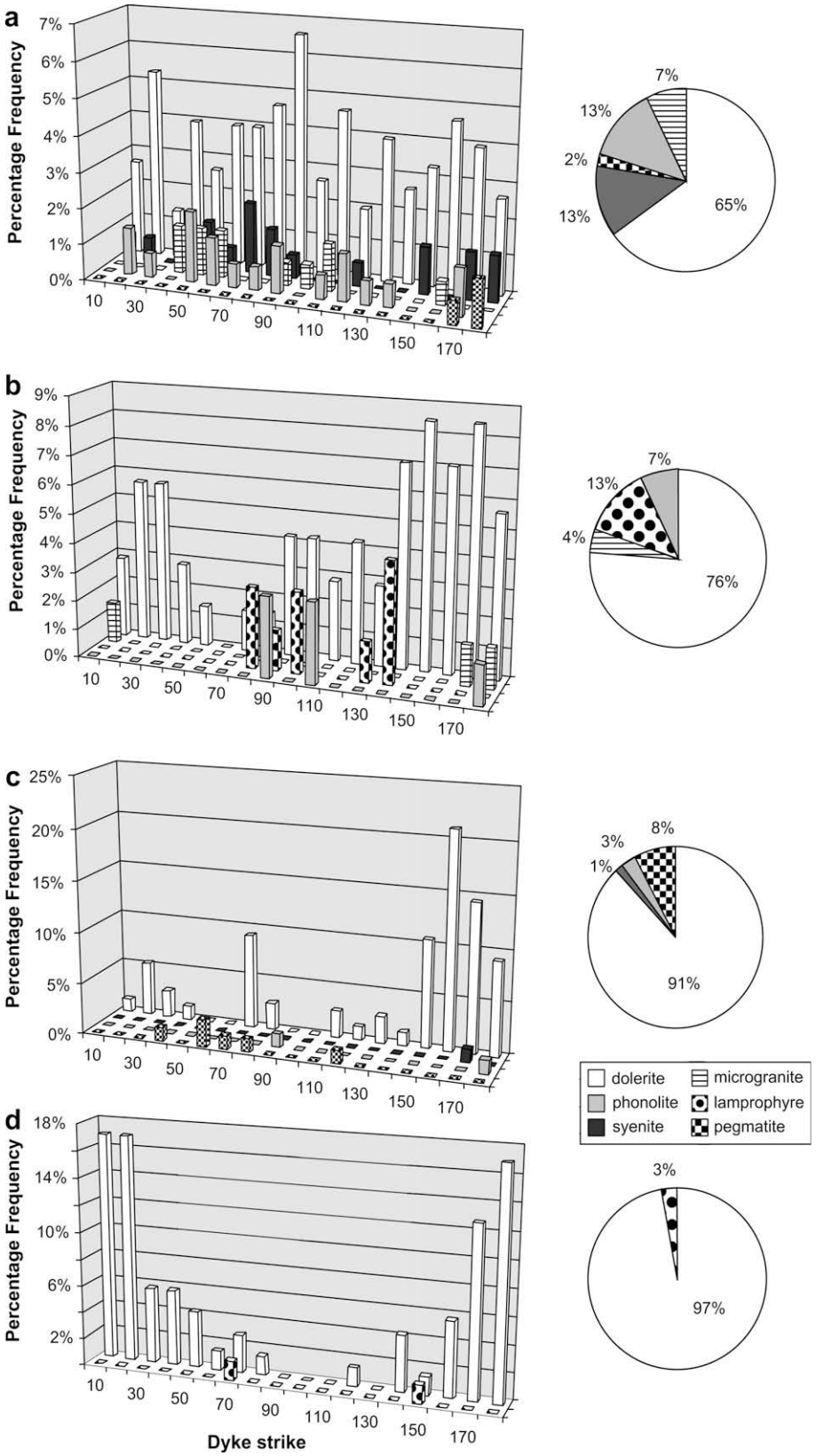

Fig. 6. Variation in percentage frequency vs. dyke trend for dykes of differing lithologies within the Straumsvola swarm: (a) the Straumsvola nepheline syenite pluton, (b) Tvora quartz syenite and immediate country rocks; and the Jutulrøra dyke swarm at: (c) Straumsvola nunataks, (d) Jutulrøra nunataks.

5.2. Variations in thickness, spacing and extension

Variations in dyke thickness and spacing within the Straumsvola dyke swarm were examined within the two syenite plutons at Straumsvola and Tvora, while comparisons within the Jutulrøra swarm were made between dykes in the country rock genisses to the south of the Straumsvola syenite pluton and those exposed 15 km southeast at Jutulrøra.

5.2.1. Thickness

Dyke thickness, measured normal to the dyke walls, was recorded for all dykes encountered in the study area. To enable an effective comparison between and within the two dyke swarms, dyke thickness was compared to normal (Gaussian), log-normal, negative-exponential and power-law distributions using cumulative frequency plots. Conformity of the data with a particular mathematical distribution is indicated by the data plotting as a straight line.

As previously described, dykes intruding the nepheline syenite pluton at Straumsvola possess an extremely wide range of trends relative to the predominantly NW–SE trend of those located outside of the pluton (Fig. 4). To determine if there is any systematic variation in the width of the Straumsvola dykes relative to their orientation, width was plotted against strike for all dykes intruding the nepheline syenite (Fig. 7). Despite the presence of several wide (>4 m) dykes striking between 90° and 150°, a moving point average analysis of the data indicates there is no significant relationship between dyke width and orientation. As a result, we have included all dykes within the Straumsvola pluton in our population distribution analysis, irrespective of trend.

In all four sub-areas, dyke thickness conforms most closely to a power-law distribution (R^2 between 0.85 and 0.97, see Table 1) obeying a single scaling relationship over the 25–19.25 m range (Fig. 8). Dykes with a thickness of less than 25 cm are under represented in all areas, which given the excellent and continuous nature of the rock exposure suggests this is a real feature of the dyke swarm and not a sampling issue. The reduced occurrence of thin dykes might be attributable to the scale limiting process of magma solidification, preferentially removing thin dykes from the distribution (Jolly, 1996).

As dyke width displays a power-law distribution, comparisons between and within the Straumsvola and Jutulrøra dyke swarms must made via the slope of the best fit lines to the cumulative distribution plots. The power-law relationship is expressed as $y = Cx^{-a}$ where y is the cumulative number; x, measure of size, in this case width, C, constant, and the exponent a, the dimension of the distribution (Pickering et al., 1995). So a power-law with fractal dimension a is seen as a straight line with slope $-a$ on a log–log plot. Using the gradients from the cumulative distribution plots, distribution dimensions vary from 1.09 to 1.48 (Fig. 9). Such high dimensions (≥1) indicate that thin dykes dominate the dyke populations relative to thick dykes, with higher dimensions indicating greater relative dominance of thin dykes. The dyke populations intruding the syenite plutons at Straumsvola and Tvora (175–178 Ma Straumsvola dyke swarm) possess the highest power-law dimensions ($a = 1.24$ and 1.47, respectively). In comparison the 206–204 Ma Jutulrøra dyke swarm has proportionately more thick dykes, with the Jutulrøra area having more thick dykes ($a = 1.09$) than the Straumsvola area ($a = 1.19$).

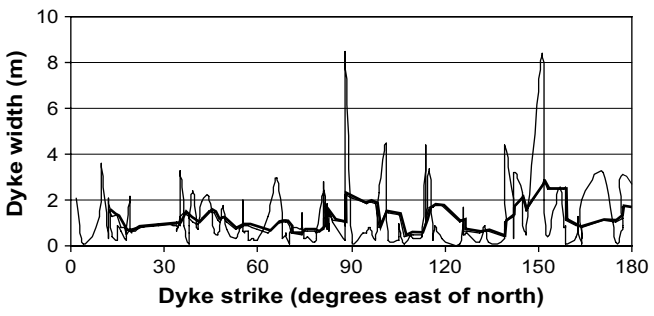

Fig. 7. A plot of dyke width against dyke trend for dykes intruding the Straumsvola nepheline syenite pluton. Heavy line is a five point moving average for the dataset.

5.2.2. Spacing

Dyke spacing was measured along two traverses through the ~205 Ma Jutulrøra dyke swarm (see Fig. 2):

- The southern ridge of Straumsvola
- The southern ridge of Jutulrøra

Dyke spacing along each traverse was measured from margin to margin of adjacent dykes, and the spacing along the traverse line corrected so that spacing normal to the mean trend of the local swarm was used in the distribution analysis, following the methodology of Jolly et al. (1998). Dyke spacing was again plotted on cumulative frequency plots and compared to normal (Gaussian), log-normal, negative-exponential and power-law distributions. The corrected dyke spacing data shows best conformity to log-normal distributions ($R^2 = 0.95$) (Fig. 10), a conclusion supported by the similarity of the median and geometric means (Table 1). The overall conformity of dyke spacing to a log-normal distribution allows the datasets to be compared by their geometric mean spacing. At the southern tip of Straumsvola, within the country rock gneiss, the Jutulrøra dyke swarm has a mean spacing of 28.9 m, whereas at Jutulrøra, 15 km to the southwest mean spacing increases to 54.3 m.

5.2.3. Extension

An approximate estimate for the amount of extension represented by emplacement of the dykes along the traverses can be estimated from the cumulative dyke thickness ($\sum t$) and length of traverse (Ln):

$$\text{Extension} = \frac{\Sigma t}{Ln} \times 100 \quad (1)$$

Extension estimates calculated from the two traverses through the Jutulrøra dyke swarm indicate a mean extension due to dyke emplacement of 2.3%. The lowest value for extension was recorded at Jutulrøra (2.06%) with the highest value (2.63%) recorded at southern Straumsvola.

6. Magnetic measurements

6.1. Anisotropy of magnetic susceptibility

Anisotropy of magnetic susceptibility (AMS) describes the orientation of magnetic minerals and its measurement has been shown to be a very sensitive technique for determining subtle fabrics related to the flow of mafic magma (e.g. Knight and Walker, 1988; Ernst and Baragar, 1992; Cañón-Tapia et al., 1996). The magnetic susceptibility tensor has six independent quantities that may be represented as three principal susceptibility magnitudes, $K_{max} \geq K_{int} \geq K_{min}$, and a corresponding set of three orthogonal principal axis directions: it may be pictured as an ellipsoid. The complete set of six parameters is required to define the ellipsoid, but it is conventional to recast the three magnitude parameters in terms of three parameters that together reflect the size, shape, and

Table 1
Statistical parameters of the thickness and spacing for dykes from specific geographical areas and traverse, respectively

Thickness Dyke swarm and Geographical area	Median (m)	Arith. mean (m)	Geom. mean (m)	Std dev. (m)	Log. std dev.	R^2 log-normal best fit line	R^2 neg-exp. best fit line	R^2 power-law best fit line	Power-law dimension
~178 Ma Straumsvola dyke swarm (Straumsvola pluton)	0.70	1.17	0.72	1.35	2.13	0.92	0.89	**0.93**	1.24
~178 Ma Straumsvola dyke swarm (Tvora pluton)	0.47	0.73	0.53	0.92	1.97	0.76	0.58	**0.85**	1.47
~204 Ma Jutulrøra dyke swarm (Straumsvola nunataks)	0.64	1.31	0.70	2.54	2.4	0.77	0.65	**0.97**	1.09
~204 Ma Jutulrøra dyke swarm (Jutulrøra nunataks)	1.06	1.78	1.09	2.41	2.38	0.85	0.82	**0.94**	1.19

Spacing Traverse	Median (m)	Arith. mean (m)	Geom. mean (m)	Std dev. (m)	Log. std dev.	R^2 log-normal best fit line	R^2 neg-exp. best fit line	R^2 power-law best fit line
~204 Ma Jutulrøra dyke swarm (South Ridge Straumsvola)	26.49	50.11	28.92	59.96	1.78	**0.95**	0.89	0.92
~204 Ma Jutulrøra dyke swarm (Jutulrøra)	54.28	90.71	54.28	104.6	2.02	**0.95**	0.92	0.91

strength (or ellipticity) of the ellipsoid. The parameters adopted here are (cf. Owens, 1974; Stevenson et al., 2007a):

$$K_{\text{mean}} = (K_{\max} + K_{\text{int}} + K_{\min})/3$$

$$L = (K_{\max} - K_{\text{int}})/K_{\text{mean}}$$

$$F = (K_{\text{int}} - K_{\min})/K_{\text{mean}}$$

A plot of the magnetic lineation L against the magnetic foliation F provides a graphical indication of the ellipsoid shape with prolate ellipsoids lying near the L-axis and oblate ellipsoids near the F-axis, whereas triaxial ellipsoids occupy the centre of the plot. Additional magnitude parameters are H and m (or μ), where

$$H = L + F = (K_{\max} - K_{\min})/K_{\text{mean}}$$

$$m = (K_{\max} - K_{\text{int}})/(K_{\text{int}} - K_{\min})$$

$$\mu = \tan^{-1} m$$

The parameter H, the total anisotropy, is a measure of the strength of the magnetic fabric. For an ellipsoid represented by a point on an L/F plot, the shape parameter m is the slope of the line

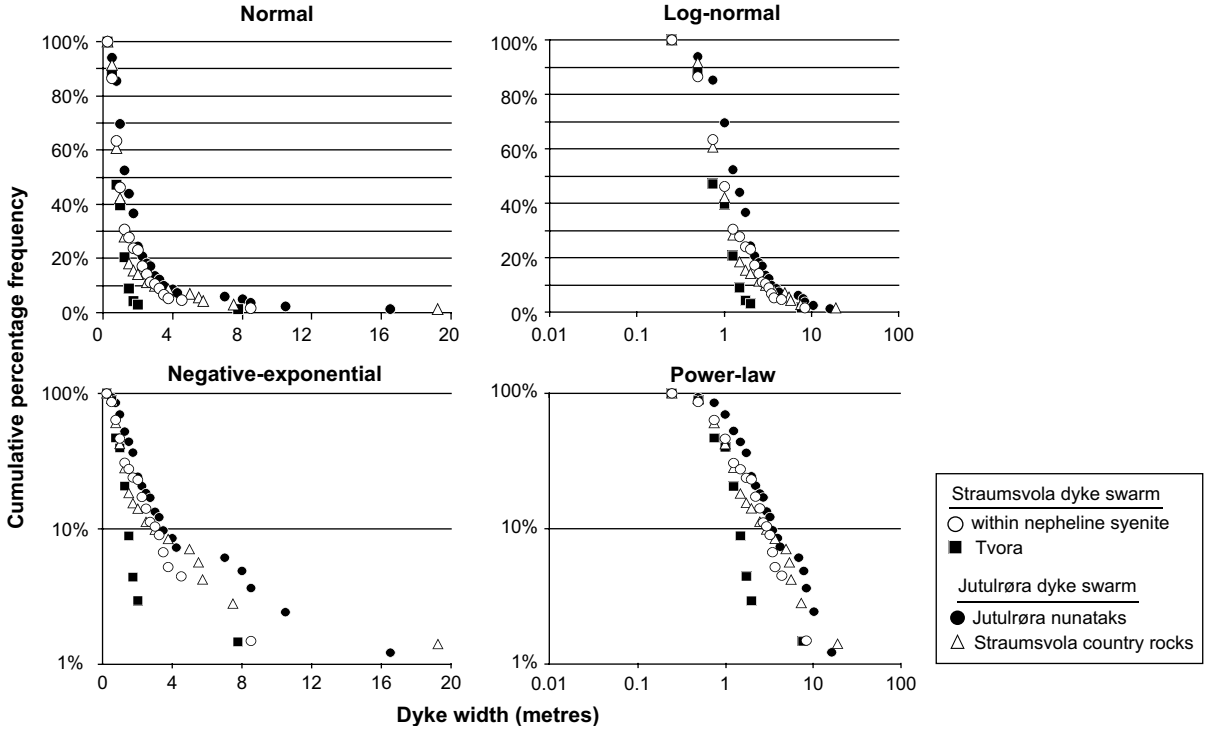

Fig. 8. Cumulative frequency plots for dyke width for four sub-areas within the Straumsvola and Jutulrøra dyke swarms, displayed on normal, log-normal, negative-exponential and power-law plots. The data from all sub-areas display a general conformity with a power-law relationship for dyke width (see text for details).

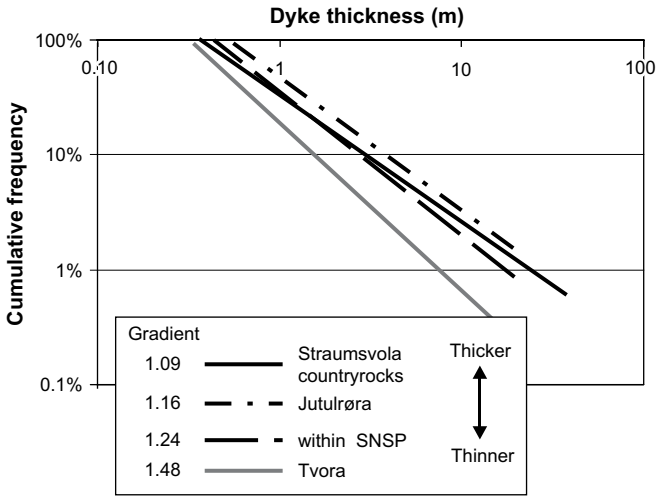

Fig. 9. Comparison of the slope of the lines of least squares fit derived from power-law cumulative frequency plot of dyke widths in Fig. 8. SNSP, Straumsvola nepheline syenite pluton.

from the origin to the point; which can also be expressed as μ, the angle of this line from the horizontal (F-axis), ranging from 0 for purely oblate to 90 for purely prolate.

The parameters outlined are preferred to the more widely used strength (P_j) and shape (T) parameters of Jelínek (1981), as they are more directly visualized in terms of the susceptibility ellipsoid, and are more appropriate to measurements made on instruments such as the torque meter and the KLY-3S Kappabridge (Stevenson et al., 2007b).

In total, 96 well-exposed dykes were block sampled from both margins, with the blocks oriented in the field using a magnetic compass. Of the 96 dykes sampled, 30 (60 block samples, one from each dyke margin) were selected on the basis of geographical coverage, orientation and relative chronology for drilling in the laboratory following the methodology of Owens (1994). The retrieved cores were measured on an AGICO kly-3s Kappabridge to determine the three mean principal axes of magnetic susceptibility K_{max}, K_{int}, K_{min} and 95% confidence ellipses (Jelínek, 1978; Owens, 2000).

Bulk susceptibility values (K_{mean}) vary from 0.28×10^{-3} to 105.3×10^{-3}, with an average K_{mean} of 34.5×10^{-3}, similar to that of other studies of mafic dykes and sills (e.g. Dragoni et al., 1997; Rapalini and de Luchi, 2000; Archanjo et al., 2000; Raposo and D'Agrella-Filho, 2000; Liss, 2003), while anisotropy strength (H) generally varies between 1 and 4% (Fig. 11a, see Table 2). The majority of samples lie within the triaxial (51%) and oblate (29%) ellipsoid fields on an L/F plot (Fig. 11b,c), however, differences in ellipsoid shape are present when the type of AMS fabric (defined by relationship of the principal axes of magnetic susceptibility relative to the dyke margin) is taken into account (see Section 6.1.1).

6.1.1. AMS fabrics

The principal axes of magnetic susceptibility K_{max}, K_{int} and K_{min} for individual block samples are generally well clustered. Based on the relative orientation of these axes to the dyke margin the AMS data can be subdivided into three commonly recognised fabric categories, denoted types A–C, plus a range of abnormal fabrics.

Type A fabrics are characterised by a good cluster of K_{max} axes lying within or close to the intrusion plane, with K_{min} axes clustering approximately perpendicular to the dyke wall (Fig. 12a). This type of fabric is referred to as a 'normal' magnetic fabric (Rochette et al., 1992) and is interpreted to be the product of magma flow where the K_{max} axis is aligned with the magma flow direction (e.g. Knight and Walker, 1988; Ernst and Baragar, 1992; Rochette et al., 1992; Raposo and D'Agrella-Filho, 2000). Samples displaying a normal AMS fabric possess an average K_{mean} of 24.5×10^{-3}, a mean $H = 2.46$, with the distribution of magnetic fabric shape parameter (μ) strongly skewed toward oblate and triaxial (Fig. 11c). Normal magnetic fabrics account for 42% of the AMS fabrics

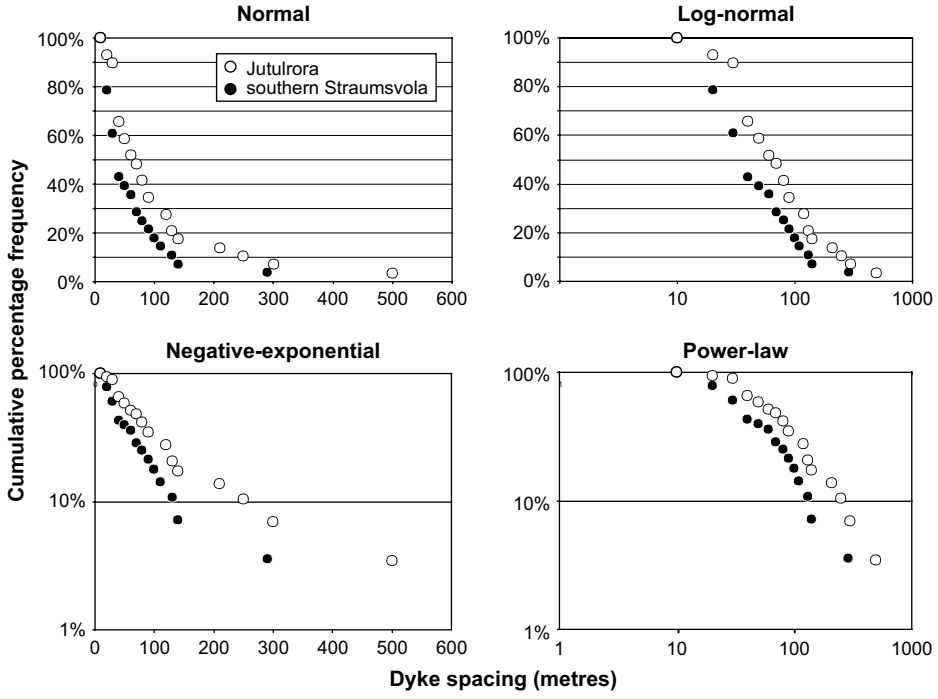

Fig. 10. Cumulative frequency plots for dyke spacing measured along two transects located at southern Jutulrøra and the south ridge of Straumsvola (see Fig. 2 for locations). Data is displayed on normal, log-normal, negative-exponential and power-law plots. General conformity exists for log-normal distribution with R^2 values >0.92.

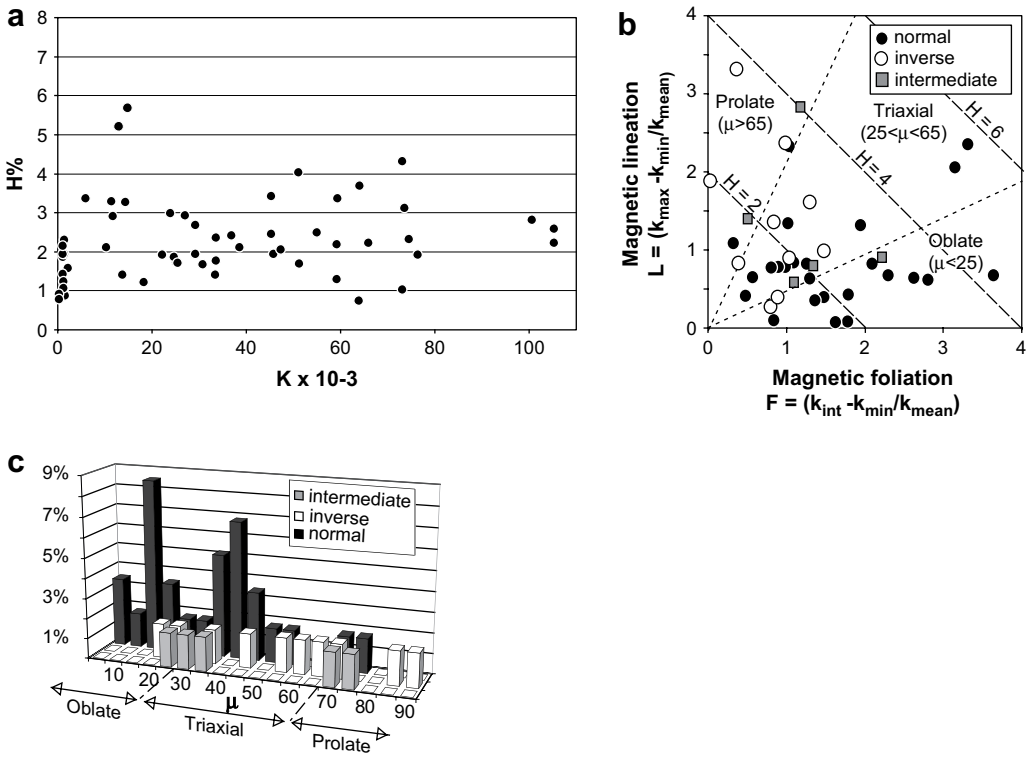

Fig. 11. Variation of anisotropy of magnetic susceptibility (AMS) parameters for block samples from H.U. Sverdrupfjella dykes. (a) *H*% (strength of anisotropy) vs. susceptibility. (b) Magnetic susceptibility data from samples displaying normal, inverse and intermediate fabrics plotted as magnetic foliation [$F = (K_{int} - K_{min})/K_{mean}$] vs. magnetic lineation [$L = (K_{max} - K_{min})/K_{mean}$], providing a graphical representation of magnetic susceptibility ellipsoid shape (μ). (c) Histogram of μ values for normal, inverse and intermediate fabrics.

measured in this study. In the nunataks of Straumsvola, Joungane, Storjoen and Tvora, 48% of magnetic fabrics are normal, whereas only 32% are normal in Jutulrøra nunataks.

Type B fabrics are characterised by a clustering of K_{max} axes perpendicular to the dyke wall with K_{int} and K_{min} lying within or close to the intrusion plane (Fig. 12b). These inverse fabrics (Rochette et al., 1992) are considered to be the product of a dominance of single domain (SD) magnetite grains (<0.1 μm), over multidomain magnetite grains with the result that K_{max} and K_{min} axes orientations become switched rendering the magnetic susceptibility fabric 'inverse' to the petrofabric. In this study, samples displaying an inverse fabric have a slightly higher average K_{mean} (39.6×10^{-3}) than that measured in samples with normal fabrics, while total anisotropy (H) similar at 2.2. The shape parameter (μ) ranges widely from oblate/triaxial to highly prolate susceptibility ellipsoids (Fig. 11c). Inverse fabrics account for 17% of the sample suite, with regional differences again found between the Straumsvola and Jutulrøra nunatak groups, where they represent 8% and 35% of the AMS fabrics, respectively.

Type C fabrics are characterised by K_{int} axes plotting approximately normal to the dyke wall, with both K_{max} and K_{min} axes lying within or close to the intrusion plane (Fig. 12c). Such fabrics are widely known as "intermediate" fabrics (Rochette et al., 1999) and are reported from other dyke swarms, being interpreted as the product of the proportional mixture of different magnetite grain sizes (Rochette et al., 1992). However, intermediate fabrics have also been identified in dykes where no magnetic grain size variation can be detected, in which case these fabrics have been variously proposed to be a result of particle rotation, secondary events (i.e. recrystallisation or hydrothermal alteration), stress-induced anisotropy due to rapid cooling, and vertical compaction of a static magma column (Rochette et al., 1991, 1999; Cadman et al., 1992; Baer, 1995; Tauxe et al., 1998; Park et al., 1988; Dragoni et al., 1997). A combination of mafic silicate subfabric and iron oxide shape fabric also results in intermediate fabrics, which has been referred to as a blended fabric (Borradaile and Jackson, 2004). Samples displaying intermediate fabrics have a similar mean total anisotropy value ($H = 2.58$) as that measured in the normal and inverse fabric and an average $K_{mean} = 35.6 \times 10^{-3}$. Intermediate fabrics account for only 8% of AMS fabrics within the study area, 10% of Straumsvola samples and 5% of Jutulrøra samples.

In this study 33% of the samples measured possess AMS fabrics that do not conform with normal, inverse or intermediate fabrics. We refer to these fabrics as abnormal. Although the configuration of the susceptibility axes relative to the plane of the intrusion within the abnormal fabrics is quite variable, they can be subdivided into two predominant types. The first (type 1 abnormal fabric) is characterised by a single, sub-horizontal, principal axis of susceptibility lying within the intrusion plane, while the remaining two axes plot equiangular about the dyke plane. Either the K_{max} or K_{min} axis may lie within the intrusion plane, with these fabric types generally associated with extreme prolate or oblate fabrics, respectively (Fig. 11d). Such fabrics account for a third of all recorded abnormal fabrics.

The most common type of abnormal fabric (type 2 abnormal fabric: 66%) is characterised by all three principal axes of susceptibility forming highly oblique angles to the intrusion plane (Fig. 11e).

6.2. Hysteresis

Twenty-nine core samples from 18 separate block samples were chosen for SIRM backfield and hysteresis analysis. The specific cores were selected to represent the main populations of AMS fabrics. The measurements were conducted at the Centre for Environmental Magnetism and Palaeomagnetism (CEMP) at the University of Lancaster, using a Molspin Nuovo Vibrating Sample Magnetometer controlled by a modified Molspin software package (Karloukovski, 2000). Plotting the ratios Mrs/Ms against Hcr/Hc on

Table 2
Summary of anisotropy of magnetic susceptibility data

Sample	n	K_{mean} 10^{-3}	H%	μ	K_{max}	K_{int}	K_{min}	L	F	Dyke	Width (m)
Z..1951.3a	10	22.2	1.92	26.4	094.24	226.56	353.22	0.64	1.29	154.68	0.54
Z..1951.3b	6	30.75	1.68	41.1	104.27	214.33	343.44	0.78	0.9	154.68	0.54
Z..1951.3c	7	51.02	4.03	67.3	246.70	028.16	121.12	2.84	1.19	060.76	0.65
Z..1951.3d	7	73.61	3.12	22.5	201.79	039.11	309.03	0.92	2.21	060.76	0.65
Z..1951.6a	12	2.12	1.58	44	202.19	086.51	304.33	0.78	0.81	158.66	5.30
Z..1951.6b	8	1.55	0.92	67.7	255.58	101.30	004.12	0.65	0.27	158.66	5.30
Z..1953.3a	7	105.3	2.22	86.9	020.58	226.29	129.12	2.11	0.11	070.69	2.94
Z..1953.3b	8	100.5	2.82	79.7	342.23	231.41	094.40	2.38	0.43	070.69	2.94
Z..1953.9a	8	1.58	0.87	40	338.65	162.24	071.01	0.4	0.47	072.74	1.86
Z..1953.9b	9	5.93	3.37	66	343.67	159.23	250.01	2.33	1.04	072.74	1.86
Z..1954.6a	7	1.15	1.42	41.4	092.63	297.25	202.10	0.67	0.75	250.84	0.90
Z..1954.6b	7	1.22	1.23	49.1	245.79	152.01	061.11	0.66	0.57	250.84	0.90
Z..1958.a	7	65.97	2.22	13.5	274.31	105.59	007.05	0.43	1.79	185.78	4.40
Z..1958.b	10	73.12	4.32	10.5	068.83	266.07	176.02	0.68	3.64	185.78	4.40
Z..1963.4a	8	12.95	5.21	33.4	248.07	141.68	341.21	2.07	3.14	173.62	1.50
Z..1963.4b	10	11.37	3.28	14	237.40	091.45	343.17	0.65	2.62	173.62	1.50
Z.1963.9a	9	13.75	1.4	47.7	302.24	055.42	191.39	0.73	0.66	254.90	0.50
Z.1963.9b	7	25.14	1.73	15.2	163.03	359.87	253.01	0.37	1.36	254.90	0.50
Z.1965.3a	8	1.46	2.3	66.2	056.38	230.51	323.03	1.59	0.7	229.67	4.38
Z.1965.3b	9	1.14	1.87	14.7	217.71	328.07	060.18	0.39	1.48	229.67	4.38
Z.1966.7a	10	10.24	2.11	57.5	265.63	101.26	008.06	1.29	0.82	059.83	2.17
Z.1966.7b	10	18.29	1.22	64.7	230.22	111.51	334.31	0.83	0.39	059.83	2.17
Z.1968.1a	8	1.23	1.07	18.5	282.04	021.64	190.26	0.27	0.8	092.84	3.38
Z.1968.1b	7	1.47	1.94	40.9	094.30	339.37	212.39	0.9	1.04	092.84	3.38
Z.1968.8a	7	14.33	3.27	34.1	218.67	013.21	106.09	1.32	1.95	108.85	2.88
Z.1968.8b	7	14.8	5.68	35.7	157.71	028.12	295.15	2.37	3.31	108.85	2.88
Z.1971.1a	7	33.59	1.76	38.5	166.42	074.02	342.48	0.78	0.98	108.75	0.40
Z.1971.1b	8	33.46	1.4	73.5	154.53	247.03	340.37	1.08	0.32	108.75	0.40
Z.1973.9a	8	0.28	0.92	6.5	222.48	082.34	337.21	0.09	0.83	180.50	0.94
Z.1973.9b	9	0.29	0.78	15.4	116.68	213.03	304.22	0.17	0.61	180.50	0.94
Z.1976.4n	9	1.10	1.93	70.2	152.83	353.06	263.02	1.42	0.51	019.86	0.12
Z.1976.4s	5	1.06	2.14	31.1	147.81	345.09	255.03	0.81	1.34	019.86	0.12
Z.1978.2a	7	23.89	2.98	16.5	298.79	132.11	042.03	0.68	2.3	131.62	0.49
Z.1978.2b	10	38.62	2.1	33.5	028.60	148.15	245.25	0.83	1.26	162.77	0.49
Z.1982.a	9	52.11	15.59	55.3	061.38	167.19	277.45	9.2	6.38	070.85	0.57
Z.1982.b	6	44.76	15.92	51.3	074.52	189.18	291.32	8.83	7.09	070.85	0.57
Z.1983.a	8	29.19	2.68	3.1	145.45	326.45	235.01	0.14	2.55	335.77	0.64
Z.1983.b	8	36.87	2.41	30.9	181.56	018.33	283.08	0.9	1.51	335.77	0.64
Z.1985.2a	5	105.27	2.59	25.66	090.47	242.40	344.15	0.84	1.75	085.68	0.63
Z.1985.2b	7	74.49	2.32	58.4	043.53	231.37	138.04	1.44	0.88	085.68	0.63
Z.1986.0a	8	33.65	2.35	53.1	190.15	006.74	100.01	1.34	1.01	074.75	16.40
Z.1986.0b	8	27.01	2.92	21.6	219.49	356.32	101.22	0.83	2.09	074.75	16.40
Z.1986.4a	9	24.71	1.87	2.5	162.85	341.05	071.01	0.08	1.79	084.82	7.90
Z.1986.4b	6	25.53	1.71	2.7	305.75	166.11	074.09	0.08	1.63	084.82	7.90
Z.1987.9a	8	11.74	2.9	51.5	136.40	341.47	137.13	1.62	1.29	117.77	8.31
Z.1987.9b	10	63.93	0.74	63.1	213.01	304.43	123.47	0.49	0.25	117.77	8.31
Z.1989.1a	11	73.09	1.02	24.9	248.08	154.29	353.60	0.32	0.7	288.75	2.12
Z.1989.1b	8	59.17	1.29	23.5	108.02	254.88	018.01	0.39	0.9	288.75	2.12
Z.1989.5a	9	59.37	3.36	67.4	264.05	157.73	355.16	2.37	0.99	282.88	0.97
Z.1989.5b	6	64.01	3.68	83.6	252.14	051.75	161.05	3.31	0.37	282.88	0.97
Z.1989.7a	10	59.28	2.19	58.1	270.13	016.51	170.36	1.35	0.84	096.80	3.78
Z.1989.8a	6	45.75	1.93	37.8	167.09	294.75	76.12	0.84	1.09	265.87	1.94
Z.1989.8b	8	45.35	3.42	12.5	248.02	250.76	078.13	0.62	2.8	265.87	1.94
Z.1990.7a	8	45.24	2.46	34.1	072.05	309.80	163.09	0.99	1.47	087.84	3.07
Z.1990.7b	11	51.29	1.69	28.8	006.78	255.04	164.11	0.6	1.09	087.84	3.07
Z.1991.1a	10	54.94	2.49	37.5	131.39	270.44	022.21	1.08	1.41	096.70	2.21
Z.1991.1b	7	47.27	2.05	56.8	246.32	117.45	355.28	1.24	0.81	096.70	2.21
Z.1992.5a	8	29.28	1.94	76	230.01	136.69	320.21	1.55	0.39	100.87	1.66
Z.1992.5b	10	76.43	1.91	89.2	076.14	252.76	346.01	1.88	0.03	100.87	1.66

n, Number of samples measured; K_{mean} = mean susceptibility; $L = (k_{max} - k_{min})/k_{mean}$; $F = (k_{int} - k_{min})/k_{mean}$; $H = (L + F)$; μ = magnetic fabric shape; oblate = 0–25; triaxial = 25–65; prolate = 65–90; Dyke = orientation dip-direction/dip.

a Day plot allows the magnetic domain size to be determined (Day et al., 1977).

The Day plot for H.U. Sverupfjella dyke swarm specimens reveals that 79% of the cores analysed fall within or on the boundary of the pseudo-single domain (PSD) field for magnetite, 4 (17%) plot within or on the boundary of multidomain magnetite, while the remaining sample fell on the boundary between both fields (Fig. 13). It is noticeable that core samples exhibiting inverse AMS fabrics show a tendency to plot toward the single domain field, whereas core samples characterised by normal AMS fabrics have Mrs/Ms values of > 1.88 and trend toward the multidomain field. The centre of the pseudo-single domain field sees an overlap of inverse, normal and intermediate fabrics.

7. Discussion

7.1. Controls on dyke emplacement

In addition to geochemical differences between the 175–178 Ma Straumsvola and 204–206 Ma Jutulrøra dyke swarms, significant

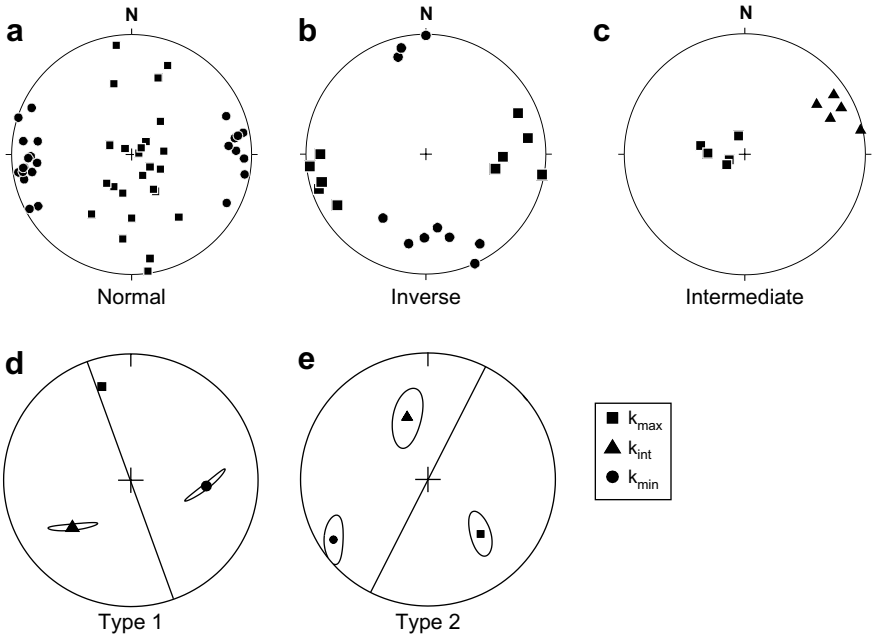

Fig. 12. Range of AMS fabrics developed within the H.U. Svedrupfjella dyke swarm. (a–c) AMS fabrics plotted relative to a common dyke orientation (N–S trending and with a vertical inclination), (a) normal fabrics, (b) inverse fabrics, and (c) intermediate fabrics. (d–e) Typical examples of type 1 and 2 abnormal fabrics, respectively.

variations in geographical extent, compositional diversity and dyke swarm structure exist.

Dykes forming the Straumsvola swarm are largely confined to the outcrop of the Straumsvola nepheline syenite pluton and its immediate country rocks, and although predominantly mafic (65%) in composition, also contains subordinate components of phonolite, pegmatite and microgranite or microsyenite. Our new Ar–Ar data reveals that the predominantly (90%) tholeiitic Jutulrøra dyke swarm was emplaced into Jutulrøra Formation gneisses prior to emplacement of the syenite plutons.

Dyke orientation varies dramatically between the two swarms, with dykes of virtually every strike direction present in the Straumsvola swarm, while the Jutulrøra swarm displays a highly restricted NNW–SSE to N–S trend. Such variation in dyke strike has been attributed to differences in magma pressure relative to the magmatic source/centre (Jolly and Sanderson, 1995) using the stress ratio (R) approach of Delaney et al. (1986). The R-ratio describes the ability of a fracture/joint to dilate and fill with magma as a function of the magma pressure (P_m), the maximum (S_H) and minimum (S_h) principal stress within the plane, and the angle (θ) between the maximum principal stress (S_H) and the normal to the dyke. Expressed as:

$$R = \frac{(P_m - S_H) + (P_m - S_h)}{(S_H - S_h)} \geq \cos 2\theta$$

Delaney et al. (1986) demonstrated that the R-ratio controls the range of pre-existing fracture orientations that are able to dilate, and has a dramatic effect on the form and emplacement style of a dyke swarm. Where $R \geq 1$ ($P_m \geq S_H$), fractures of any orientation are able to dilate, whereas when $1 > R > -1$, the range of fracture orientations able to dilate becomes increasingly restricted until $R = -1$, when only fractures parallel to the maximum principal stress (S_H) are able to dilate and magma pressure (P_m) is equal to the minimum principal stress (S_h).

Dyke opening direction (α), measured relative to the normal to the dyke wall (Fig. 14), has also been related to the R-ratio with specific dyke opening behaviour predicted (Jolly and Sanderson, 1995). When $R > 1$ ($P_m > S_H$), dykes of any orientation can dilate and fill, with highly variable opening directions within the dyke population, whereas when $R = 1$ ($P_m = S_H$), dykes of any orientation may form, but their opening direction is highly restricted and is parallel to the minimum principal stress direction (S_h). Where $1 > R > -1$ the range of dyke orientations is restricted, while opening direction is dependent on the orientation of the facture. In the specific case of $R = 0$, opening directions are generally oblique to S_h. When $R = -1$, only fractures normal to S_h are able to dilate with an opening direction parallel to S_h.

A basic comparison of our data with the emplacement models of Delaney et al. (1986) and Jolly and Sanderson (1995) allows relative estimates to be made for the R-ratio between the Straumsvola and Jutulrøra dyke swarms. The wide range of dyke orientation within the Straumsvola swarm suggest an R-ratio of $R \geq 1$, whereas the highly restricted orientation of dykes in the Jutulrøra swarm suggest an R-ratio of $1 > R > -1$, i.e. magma pressure was greater within the 175–178 Ma Straumsvola swarm than the 204–206 Ma Jutulrøra dyke swarm.

Further refinement of the estimated R-ratio may be made by considering the opening direction of the dykes within the

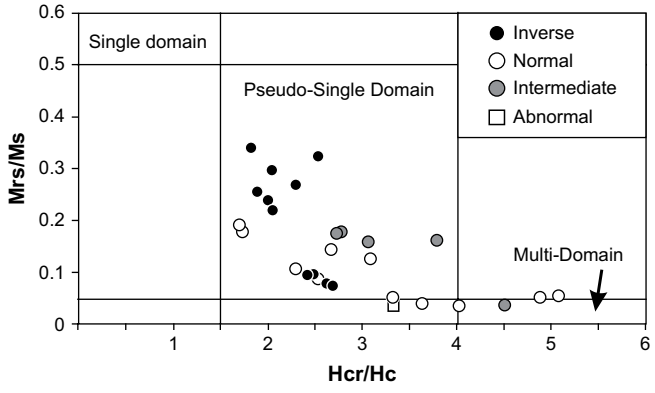

Fig. 13. Hysteresis parameters for normal, inverse, intermediate and abnormal fabrics from the H.U. Svedrupfjella dyke swarm displayed in a Day plot (Day et al., 1977).

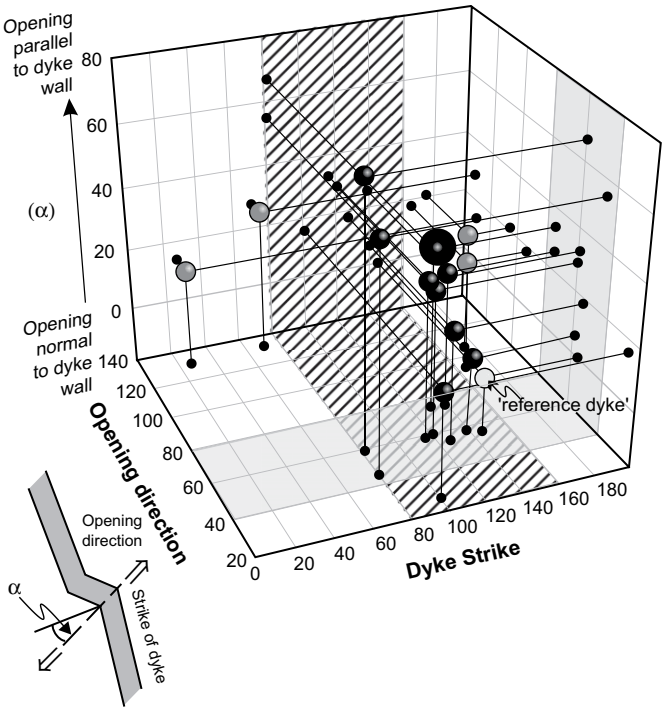

Fig. 14. A plot of dyke strike, opening direction, and opening obliquity (α) of individual dykes intruding the Straumsvola nephelene syenite pluton. Black points represent dykes interpreted to have intruded while R-ratio = 1 (wide range of orientation but highly restricted open direction), light grey point, reference dyke displaying orthogonal opening; mid grey points, dykes displaying significantly different opening directions. The grey shaded and hatched areas highlight the range of opening direction and dyke strike, respectively, inferred to have been emplaced when $R = 1$.

Straumsvola swarm. Within the pluton, dyke opening directions derived from exposed offsets reveal a predominantly northeast–southwest directed opening direction, while four dykes display variable opening directions between east–west to southeast–northwest. Plotting the opening direction, dyke strike, and angle between opening direction and the perpendicular to dyke strike (α) of individual dykes on an X, Y, Z graph provides a useful method for assessing the relationship between these three variables (Fig. 14). The majority of dykes where an opening direction was observed display an approximate northeast–southwest direction. One of these dykes displays a perfectly orthogonal opening direction ($\alpha = 0$) and is used as a comparative reference for dyke orientation and opening direction (strike 146°, opening direction 056°). It is apparent from Fig. 14 that several dykes share a fairly consistent opening direction (sub-parallel to the reference dyke's opening direction of 056°) regardless of dyke orientation, including two highly oblique, east–west trending dykes. These dykes show a linear increase in angle α with increasing obliquity of dyke strike to the ideal reference dyke orientation. Such a relationship is consistent with a dyke emplacement model where the R-ratio = 1 (Delaney et al., 1986). An implication of this model is that when $R = 1$, the opening direction is parallel to the minimum principal stress (S_h) direction, thus the average opening direction recorded within the majority of dykes within the Straumsvola dyke swarm (N57°E) records the minimum principal stress direction at the time of dyke emplacement.

Four dykes displaying northwest–southeast to east–west opening directions have strikes outside the range of those displaying a consistent NE–SW opening direction, and display low to moderate opening obliquity ($\alpha = 14$–$28°$). This difference in opening direction might indicate that these dykes were either intruded at a time when the principal stress directions differed or alternatively they were intruded under differing R-ratio conditions. Examination of 44 localities where cross-cutting dyke relationships are exposed reveals no consistent relationship between relative chronology and mafic dyke orientation within the pluton, suggesting that there is no systematic temporal difference in the dyke population. Thus it appears more likely that the explanation for these variations in dyke opening directions is a change in R-ratio during dyke emplacement. When $R = 0$ a more restricted range of dyke orientations are able to dilate but their opening directions are generally oblique to the minimum principal stress direction. Such a relationship is consistent with the data from the four dykes showing E–W to SE–NW opening directions. We therefore propose that the form and emplacement style of the Straumsvola dyke swarm is the product of a variation in magma pressure causing the R-ratio to vary between 1 and 0.

Dyke orientation within the Jutulrøra dyke swarm is locally much more restricted suggestive of an R-ratio $0 > R > -1$, although across the study area the average dyke trend fans from NNW–SSE to N–S. Only four dykes, all encountered within the N–S trending component of the swarm, display evidence for their opening direction making a more refined estimate for dyke swarm R-ratio difficult. Two NNE–SSW striking dykes display roughly E–W opening directions, which would be consistent with a perpendicular opening direction relative to the mean trend of the Jutulrøra dyke swarm at Jutulrøra nunatak.

Two additional dykes with atypical orientations and opening directions were also encountered. A N140°E striking dyke displaying a low-obliquity opening direction of 028–208°, is theoretically consistent with predicted dyke orientation and opening directions when $R = 0$ (Jolly and Sanderson, 1995). The second dyke is strongly atypical of the Jutulrøra swarm, trending N55°E and displaying a near orthogonal opening direction of 148°. This dyke orientation is similar to a late stage set of mafic dykes cross-cutting the Jutulrøra dyke swarm adjacent to the Straumsvola nepheline syenite pluton or the c.190 Ma dykes in the Ahlmannryggen region to the west of the Jutulstraumen icestream (Riley et al., 2005) and thus may be younger and unrelated. However, the locally poor quality exposure obscures the cross-cutting relationship between the N55°E dyke and the main Jutulrøra dyke swarm.

In addition to the apparent radiation of the Jutulrøra dyke swarm within the study area, the structural data and presented in this paper identifies an along strike variation in dyke distribution away from the swarm's apparent point of convergence. From Straumsvola to Jutulrøra nunataks the dyke swarm exhibits:

1. An increase in dyke spacing (from 30.2 m to 57.53 m).
2. An increase in the proportion of thick dykes.
3. A slight decrease in extension (2.6% to 2.06%).

A similar pattern of dyke form and distribution exists in the Mull dyke swarm of the British Tertiary Igneous Province, which has been interpreted as a product of thin dykes either merging or dying out with increasing distance away from an igneous centre (Jolly and Sanderson, 1995) thus overcoming limitations of magma flow within a thin dyke (Rubin, 1993). We interpret the distribution of the Jutulrøra dyke swarm in the same manner.

7.2. Magma flow within Straumsvola and Jutulrøra dyke swarms

The close spatial and temporal relationship of the Straumsvola dyke swarm with the nepheline syenite pluton suggests the magma was locally sourced with the magma transport direction being predominantly vertical. In contrast, the form and distribution of dykes within the Jutulrøra swarm are indicative of magma flowing from north to south away from an inferred source area centred at the convergence of the apparent dyke swarm fan (e.g. northern

Jutulstraumen rift to the northwest of Straumsvola nunataks). In such a scenario, magma might be expected to flow vertically above and immediately adjacent to the source area, with flow becoming increasing lateral away from the source. Such flow patterns have been identified within giant dyke swarms associated with mantle plumes (Ernst and Baragar, 1992) as well as smaller more localised magma centres (Archanjo et al., 2000; Callot et al., 2001). Our AMS results allow us to test these hypotheses.

The K_{max} axes of normal AMS fabrics are generally accepted to be parallel to the magma flow direction within a dyke or sill (Knight and Walker, 1988; Ernst and Baragar, 1992; Rochette et al., 1992; Raposo and D'Agrella-Filho, 2000). Within the normal fabrics identified in the study area, 58% display steeply inclined K_{max} axes relative to their sub-vertical dyke wall, while the remaining 42% possess sub-horizontal K_{max} axes. In all cases where normal fabrics were measured from both margins of a dyke, the individual K_{max} axes are consistent, i.e. they are either both sub-vertical or both sub-horizontal, giving us confidence that the normal fabrics and the orientation of K_{max} represents the direction of magma flow.

Normal fabrics derived from dykes within the Straumsvola swarm (intruding the syenite plutons at Straumsvola and Tvora) are dominated (82%) by steeply inclined K_{max} axes suggesting magma flow was vertical (Fig. 15). Although independent field evidence for magma flow is limited, this interpretation is corroborated for dyke Z.1971.1 near the summit of Straumsvola, where sub-vertically plunging stretched amygdales are exposed.

The remaining 18% of normal fabrics display sub-horizontal K_{max} axes, and are found in subordinate set of ENE–WSW trending dykes. Similar orientation dykes displaying sub-horizontal K_{max} axes cross cut dykes of the Jutulrøra swarm in the country rock gneisses to the south of the pluton margin. We interpret these ENE–WSW trending dykes as having facilitated sub-horizontal magma flow, an interpretation corroborated at dyke Z.1963.4 by stretched amygdales, the long axes of which are parallel to the K_{max} axis derived from the northern margin of the dyke. Although, these ENE-trending dykes are a component of the Straumsvola dyke swarm they differ in that magma appears to have been emplaced laterally.

K_{max} axes derived from dykes from the Jutulrøra swarm exhibit striking geographical differences. Within the Straumsvola nunatak area, dykes within the Jutulrøra swarm display consistent vertical K_{max} axes suggesting magma flow was vertical. Fifteen kilometres to the south at Jutulrøra nunataks, only three of 10 dykes analysed displayed normal fabrics. Two of those dykes possess AMS fabrics displaying shallowly inclined to sub-horizontal K_{max} axes, while the remaining dyke has a sub-vertical K_{max}. Such limited data makes generalisations regarding overall magma flow within the Jutulrøra dyke swarm difficult, although clearly the presence of two representative dykes displaying sub-horizontal K_{max} suggests that lateral magma flow might be an important feature of the dyke swarm.

Of the remaining seven dykes, inverse fabrics were recorded in 60% of their margins, with 71% of these inverse fabrics displaying sub-horizontal K_{min} and K_{max} axes. The origin of inverse fabrics has been attributed to either magnetite grain size or the presence of low susceptibility paramagnetic or antiferromagnetic mineral species (Rochette et al., 1999). In the case of the Jutulrøra dyke swarm samples the relatively high average K_{mean} value (39.6×10^{-3}) suggests that the carrier mineral is magnetite. Therefore, it appears that an abundance of single domain magnetite grains, may be responsible for the presence of the inverse fabrics. Plotting the ratios Mrs/Ms against Hcr/Hc, derived from SIRM backfield and hysteresis analsyis, on a Day plot (Day et al., 1977) (Fig. 13) reveals that samples displaying inverse fabrics plot within the pseudo-single domain field, albeit trending toward the single domain field whereas normal fabrics are grouped and trend toward the multidomain field, with intermediate fabrics plotting within an area of overlapping AMS fabrics. These data reveal that the inverse fabrics are not the result of a uniform size population of single domain magnetite grains. Instead, it may be possible that the spatial variation of AMS fabrics within the psuedo-single domain

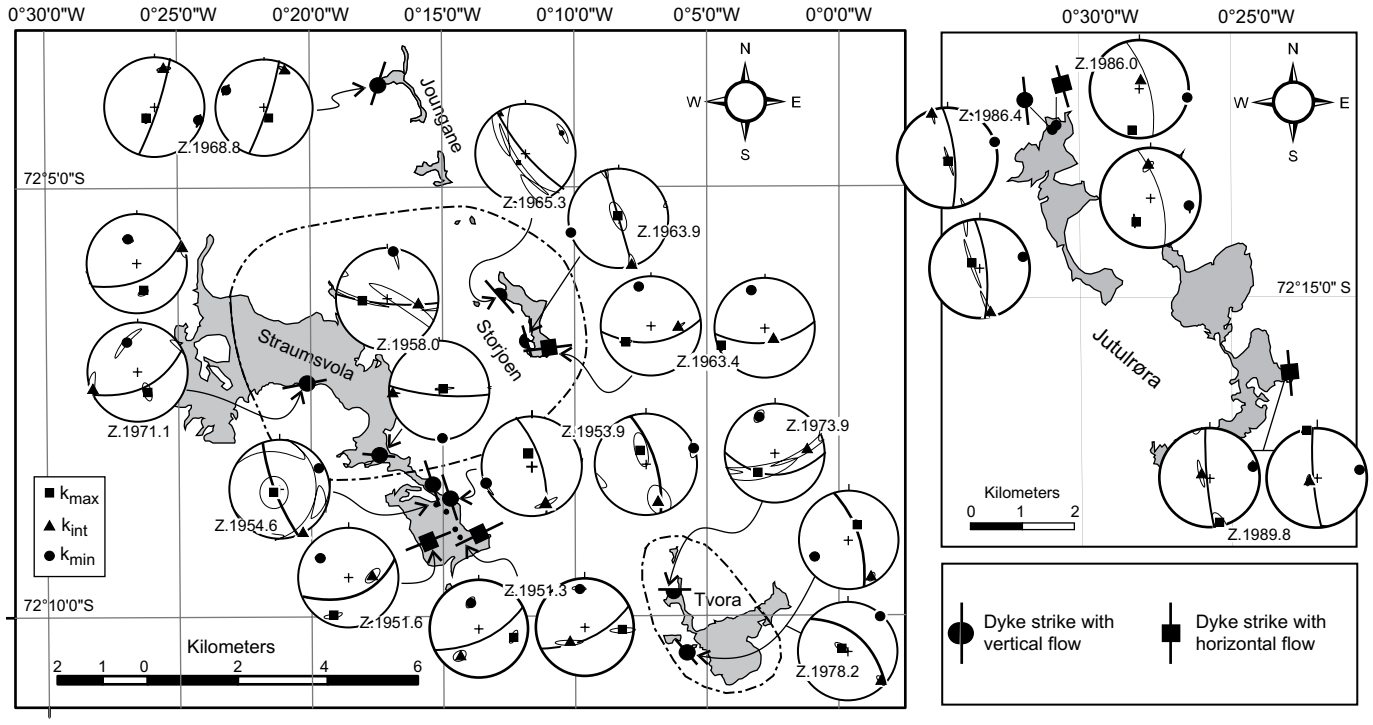

Fig. 15. Location maps for sampled dykes displaying normal AMS fabrics in one or both margins. Relative magma flow has been interpreted as either horizontal or vertical flow based on the orientation of K_{max}. Principal axes of susceptibility with 95% confidence limits for each sample are plotted on stereograms.

field of the Day plot is the product of proportional mixing of single and multidomain magnetites, which can result in the development of a range of fabrics the end members of which are inverse and normal (Rochette et al., 1992). If the inverse fabrics in the Jutulrøra dyke swarm are a result of the switching of K_{max} and K_{min} axes due to the predominance of SD magnetite within a mixed grain size distribution, we suggest that the dominant sub-horizontal attitude of these axes supports the limited normal AMS fabric data that magma flow within the swarm was predominantly lateral, i.e. parallel to the measured K_{min} axis of the inverse fabrics. This interpretation is corroborated in one of the dykes possessing an inverse fabric, dyke Z.1989.5, which displays sub-horizontally stretched amygdales suggesting magma flow was parallel to the K_{min} axis of the inverse fabric.

The pattern of K_{max} axes, and interpretation of inverse fabrics, within the Jutulrøra dyke swarm suggests that magma ascended vertically from a source area within the Straumsvola region and flowed laterally to the south. This data is consistent with the form and distribution of dykes within the swarm and air geophysical evidence which indicates the presence of a potential magma source beneath Straumsvola in the form of a significant mafic body (Ferraccioli et al., 2005a,b).

7.3. Regional tectonics

The Mesozoic dyke swarms exposed in Dronning Maud Land, the Antarctic component of the Karoo large igneous province, were emplaced over a wider time span than is currently known in southern Africa. In H.U. Sverdrupfjella, the mafic dykes reported in this contribution were emplaced between 206–204 Ma and 178–175 Ma, extending the already wide range of reported ages from the Ahlmannryggen region, where $^{40}Ar/^{39}Ar$ dates of 192 ± 8 Ma (Wolmarans and Kent, 1982), as well as c.190 Ma and 178 Ma for structurally and geochemically distinct dyke emplacement events (Riley et al., 2005) have been reported. In Vestfjella, Zhang et al. (2003) reported ages of c.193 Ma for a dolerite dyke from Basen, while the majority of Vestfjella dykes were considered to be c.177 Ma based on geochemical correlation with well-dated lava flows. An age of 176.6 ± 0.5 Ma was also reported from a dolerite dyke in Kirwanveggen (Zhang et al., 2003).

Structural and AMS data from the 206–204 Ma Jutulrøra dyke swarm indicates that it was locally sourced from a long-lived igneous centre in the vicinity of Straumsvola, while the apparent fan of dyke orientations within the swarm is suggestive of a partially exposed radiating dyke swarm. The oldest Mesozoic dykes identified in the Ahlmannryggen are ~N70°E striking Group 1 dykes (Riley et al., 2005) which form an excellent geometrical fit to the apparent radiating Jutulrøra swarm (Fig. 16a) and are, in part, attributed to the role of a mantle plume. However, the Ahlmannryggen dykes are, at 190 Ma, significantly younger than the Jutulrøra dyke swarm. While it is tempting to relate the emplacement of these dykes to a prolonged period of doming and radial fracturing centred on the northern Jutulstraumen icestream, dyke emplacement at ~204 Ma is ~25 Myr prior to the main Karoo event and although it is now generally believed that CFB provinces can have a prolonged history (Jerram and Widdowson, 2005; Riley et al., 2005) the timescale in Dronning Maud Land is too lengthy to make robust correlations with plume involvement prior to 190 Ma.

Despite the extended age range of dykes within western Dronning Maud Land, all the areas are linked by a dyke emplacement event between 175 and 178 Ma. In Vestfjella, the majority of dykes (80%) share a restricted NE–SW trend (Spaeth, 1987),

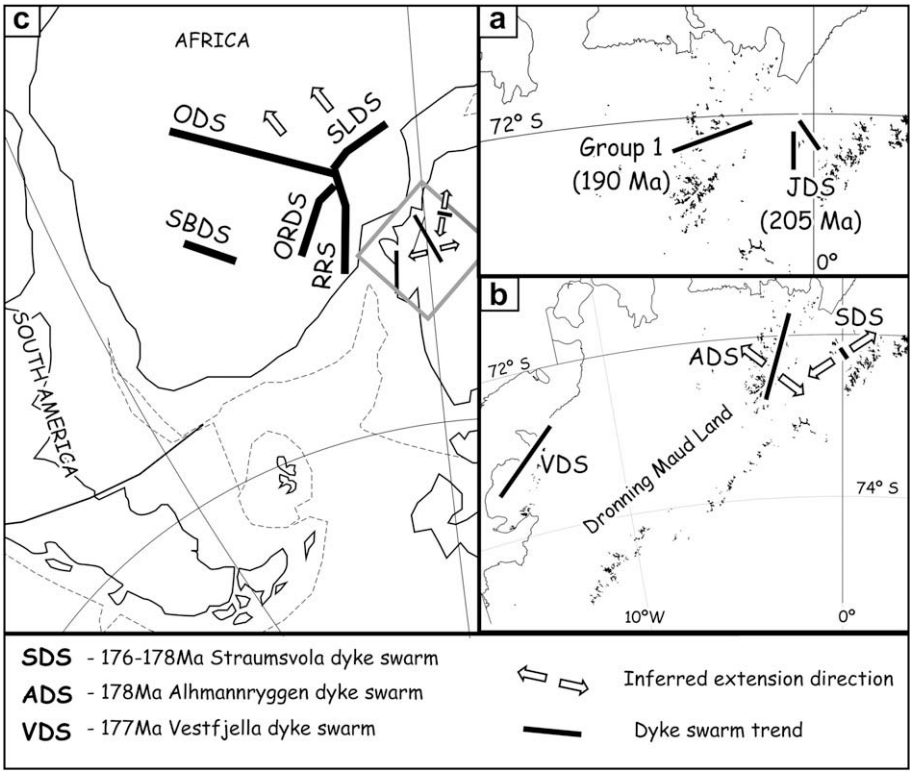

Fig. 16. (a) Map of western Dronning Maud Land displacing the location and orientation of ~205 Ma Jutulrøra dyke swarm and 190 Ma Ahlmannryggen dykes. (b) Present day western Dronning Maud Land displaying general orientation of 175–178 Ma radiating dyke swarms and their extension directions. (c) 178 Ma Gondwana reconstruction showing the relative trends of the giant dyke swarms of southern Africa (dyke swarms and inferred extension direction for the ODS & SLDS from Le Gall et al., 2002), relative to radiating dykes of western Dronning Maud Land. ODS, Okavango dyke swarm; SLDS, Sabi-Limpopo dyke swarm; ORDS, Olifants River dyke swarm; RRS, Rooi Rand dyke swarm; SBDS, southern Botswana dyke swarm. Grey box highlights the approximate extent of adjacent western Dronning Maud Land maps.

approximately parallel to the present day continental margin, while in the Ahlmannryggen the 178 Ma dykes trend NNE–SSW and were emplaced in response to an NW–SE oriented minimum principal stress (present day coordinates) (Riley et al., 2005). In H.U. Sverdrupfjella, although the newly defined Straumsvola dyke swarm displays highly varied dyke orientations due to inferred high magma pressure within a local igneous centre, structural data indicates it was emplaced within a stress regime where the a minimum principal stress was oriented N57°E (present day coordinates).

Plotting the orientation of the 175–178 Ma dyke swarms and minimum principal stress directions on a 178 Ma reconstruction of Gondwana (Fig. 16b, c), it is evident that the Vestfjella and Ahlmannryggen dyke orientations converge toward a position located near the present day continental margin of western Dronning Maud Land, while inferred minimum principal stress directions appear to form part of a radial stress system about the same location. We propose that these features are consistent with the c.178 Ma western Dronning Maud Land dykes forming a true radiating dyke swarm centred within the commonly proposed Karoo plume head (Fig. 16c).

In southern Africa, a giant radiating dyke swarm composed of the Okavango (ODS), Sabi-Limpopo (SLDS), Lebombo (LDS) and Olifants River dyke swarms (ORDS), converges at Nuanetsi, southern Zimbabwe (Fig. 16c). All the dyke swarms are considered to have been emplaced between 180 and 175 Ma (Watkeys, 2002), with precise $^{40}Ar/^{39}Ar$ dates suggesting an emplacement age for the ODS and SLDS of c.178 Ma (Elburg and Goldberg, 2000; Le Gall et al., 2002; Jourdan et al., 2004), contemporaneous with those in the conjugate Dronning Maud Land margin. The confluence of giant dyke swarms is generally interpreted to indicate the presence of a rift triple junction above the site of a former mantle plume (e.g. Burke and Dewey, 1972; White and McKenzie, 1989; Storey, 1995; Ernst and Buchan, 1997; Elliot and Fleming, 2000), although this interpretation has recently been challenged by geochronological and structural evidence from the ODS and SLDS suggesting that both swarms were emplaced into long-lived zones of structural weakness (Le Gall et al., 2002; Jourdan et al., 2004), while estimates for palaeostress direction suggest the dyke swarms were emplaced into a unidirectional stress field (Le Gall et al., 2005). Le Gall et al. (2002, 2005) and Jourdan et al. (2004) suggest that the apparent radiating geometry of the Karoo giant dyke swarms is a consequence of structural inheritance and question the appropriateness of assigning a mantle plume model to explain their pattern.

Despite these reservations, and more general challenges to the mantle plume model (e.g. Foulger, 2002), several criteria are present in the Karoo LIP that are commonly used to determine the former presence of a mantle plume (Campbell, 2001). The physical characteristics of the LIP, i.e. large volume of continental flood basalts (CFB) ($>2\times10^6$ km^3; Elliot et al., 1999), erupted over a short time period (184–179 Ma; Duncan et al., 1997), have led many workers to conclude that only a significant thermal anomaly in the mantle could have generated such large melt volumes (e.g. Cox, 1989; Ellam and Cox, 1991; Sweeney et al., 1994). Although the geochemistry of most of the Karoo CFBs cannot be directly related to a plume (Hawkesworth et al., 1999), an increasing body of geochemical and isotopic evidence reveals the presence of picrites and ferropicrites, in southern Africa and Dronning Maud Land, respectively, interpreted as being small volume, anomalously hot and deep melts derived from some component of a mantle plume (e.g. Ellam and Cox, 1991; Ellam et al., 1992; Sweeney et al., 1994; Luttinen et al., 1998; Riley et al., 2005). In addition to physical characteristics of the volcanism and geochemical evidence, Karoo magmatism appears to have coincided with domal uplift at c. 180 Ma (Cox, 1989; White and McKenzie, 1989).

Although the appropriateness of interpreting the giant radiating dyke swarms of southern Africa as a response to crustal doming has been questioned, our structural data from western Dronning Maud Land provides strong support for the existence of a true radial dyke swarm (i.e. minimum principal stress concentric about the convergence point of the dyke swarms), albeit small volume, within the Karoo LIP between 175 and 178 Ma, with geochemical and isotopic data revealing that some dykes within this radiating swarm contain melts derived from a mantle plume (Riley et al., 2005).

Given the broad range of criteria supporting the role of a mantle plume in generation of the Karoo LIP, we support previous tectonic interpretations that place the giant dyke swarms of southern Africa within a mantle plume context. However, the more complicated emplacement tectonics of at least some of these giant African dyke swarms is demonstrably a product pre-existing zones of crustal weakness that may have controlled the location of magma pathways (Le Gall et al., 2002, 2005) by which plume-related melt migrated. We concur with Le Gall et al. (2002) that although the intersection of these dyke swarms at Nuanetsi may have formed a locus for magmatic activity, it may not mark the centre of the surface doming associated with the Karoo plume. We suggest that the radiating dyke swarm of western Dronning Maud Land indicates that the centre of uplift may have been located along the eventual continental margins of Africa and Antarctic, which if correct, would mean that the giant dyke swarms of the Karoo were situated off centre of the surface doming, providing a potential explanation for the unexpected palaeostress estimates associated with the ODS and SLDS.

8. Conclusions

The Mesozoic dykes of the H.U. Sverdrupfjella and Ahlmannryggen regions of western Dronning Maud Land record a prolonged and complicated tectonomagmatic history, with the Straumsvola area in particular acting as a long-lived magmatic centre. $^{40}Ar/^{39}Ar$ whole rock geochronology reveals the presence of two temporally distinct Mesozoic dyke swarms within the H.U. Sverdrupfjella region:

The Jutulrøra dyke swarm was emplaced into basement gneisses of Sverdrupfjella Group at ~204 Ma. Dyke trend within the swarm fans from NW–SE at Straumsvola to N–S at Jutulrøra, with both dyke width and dyke spacing increasing away from the inferred convergence of the dykes. AMS data indicates magma flow was sub-vertical in the vicinity of Straumsvola, whereas in Jutulrøra, 15 km to the south, more limited data suggests that lateral flow may have dominated. The combined structural and AMS characteristics of the Jutulrøra dyke swarm are consistent with it be sourced from a local igneous centre within the vicinity of Straumsvola.

The Straumsvola dyke swarm was predominantly emplaced into syenite plutons exposed at Straumsvola and Tvora between 178 and 175 Ma. The form and distribution of the Straumsvola swarm suggests that high magma pressure (P_m) associated with the igneous centre at Straumsvola controlled emplacement. Relative estimates for P_m using the R-ratio of Delaney et al. (1986) indicate that P_m was approximately equal to the maximum principal stress ($R=1$), with the dyke swarm characterised by a diverse range of orientations but with a narrow range of opening directions, the mean of which (N57°E) is inferred to be parallel to minimum principal stress direction during emplacement. AMS data indicates magma flow was vertical, a conclusion corroborated by limited field observations. Late stage phonolite dykes cross-cutting the mafic component of the Straumsvola dyke swarm were emplaced at 171 Ma, providing an lower age constraint for magmatism within the Straumsvola intrusive suite.

On a regional scale, dyke emplacement occurred throughout western Dronning Maud Land between 178 and 175 Ma, with the Straumsvola dyke swarm forming one component of a radiating dyke swarm that also contains the 177 Ma, NE–SW trending dykes of Vestfjella, and the 178 Ma, NNE–SSW trending dykes in Ahlmannryggen. The Vestfjella and Ahlmannryggen dyke swarms apparently converge near the present day continental margin of Dronning Maud Land, north of the Jutulstraumen icestream, while estimates for minimum principal stress directions associated with emplacement of the Straumsvola and Alhmannryggen dykes indicate it was concentric about the inferred point of dyke swarm convergence. This newly recognised c.178 Ma radiating dyke swarm in western Dronning Maud Land is consistent with a mantle plume model for the generation of the Karoo LIP.

The magma flow within the apparently radiating Jutulrøra dyke swarm suggests that a local igneous centre existed in the vicinity of Straumsvola as early as ~204 Ma. Although, plume involvement in the Karoo LIP has been extended back to 190 Ma (Riley et al., 2005), Jutulrøra dyke swarm emplacement occurred ~15 Myr prior (~25 Myr prior to the main Karoo event) which is too lengthy to make robust correlations with plume involvement.

Acknowledgements

Field support was provided by the British Antarctic Survey air unit and the staff of SANAE research station. Steve Hinde and Rob Smith are thanked for field assistance, while John Huard (Oregon State university) provided assistance with $^{40}Ar/^{39}Ar$ analysis. We are grateful to M. Egydio-Silva and an anonymous reviewer for comments leading to an improvement of the original manuscript.

References

Archanjo, C.J., Trindade, R.I., Macedo, J.W.P., Araújo, M.G., 2000. Magnetic fabric of a basaltic dyke swarm associated with Mesozoic rifting in northeastern Brazil. Journal of South American Earth Sciences 13, 179–189.

Baer, G., 1995. Fracture propagation and magma flow in segmented dykes: field evidence and fabric analyses, Makhtesh Ramon, Israel. In: Baer, G., Heimann, M. (Eds.), Physics and Chemistry of Dykes. Balkema, Rotterdam, pp. 125–140.

Borradaile, G.J., Jackson, M., 2004. Anisotropy of magnetic susceptibility (AMS): magnetic petrofabrics of deformed rocks. In: Martin-Hernandez, F., Lünenburg, C.M., Aubourg, C., Jackson, M. (Eds.), Magnetic Fabric: Methods and Applications. Geological Society London, Special Publication, 238, pp. 99–360.

Burke, K., Dewey, J.F., 1972. Plume generated triple junctions. Key indicators in applying plate tectonics to old rocks. Journal of Geology 81, 403–433.

Cadman, A.C., Park, R.G., Tarney, J., Halls, H.C., 1992. Significance of anisotropy of magnetic-susceptibility fabrics in Proterozoic mafic dykes, Hopedale Block, Labrador. Tectonophysics 207, 303–314.

Callot, J.-P., Geoffroy, L., Aubourg, C., Pozzi, J.P., Mege, D., 2001. Magma flow directions of shallow dykes from the East Greenland volcanic margin inferred from magnetic fabric studies. Tectonophysics 335, 313–329.

Cañón-Tapia, E., Walker, G.P.L., Herrero-Bervera, E., 1996. The internal structure of lava flows – insights from AMS measurements 1: near vent a'a. Journal of Volcanology and Geothermal Research 70, 21–36.

Cox, K.G., 1989. The role of mantle plumes in the development of continental drainage patterns. Nature 342, 873–877.

Campbell, I.H., 2001. Identification of ancient mantle plumes. In: Ernst, R.E., Buchan, K.L. (Eds.), Mantle Plumes: Their Identification Through Time, Boulder Colorado. Geological Society of America Special Paper 352, pp. 2–21.

Day, R., Fuller, M., Schmidt, V.A., 1977. Hysteresis properties of tanomagnetites – grain size and compositional dependence. Physics of the Earth and Planetary Interiors 13, 260–267.

Delaney, P.T., Pollard, D.D., Ziony, J.I., McKee, E.H., 1986. Field relationships between dikes and joints – emplacement processes and paleostress analysis. Journal of Geophysical Research 91, 4920–4938.

Dragoni, M., Lanza, R., Tallarico, A., 1997. Magnetic anisotropy produced by magma flow: theoretical model and experimental data from Ferrar dolerite sills (Antarctica). Geophysical Journal International 128, 230–240.

Duncan, R.A., Hooper, P.R., Rehacek, J., Marsh, J.S., Duncan, A.R., 1997. The timing and duration of the Karoo igneous event, southern Gondwana. Journal of Geophysical Research 102, 18127–18138.

Elburg, M., Goldberg, A., 2000. Age and geochemistry of Karoo dolerite dykes form northeast Botswana. Journal of African Earth Sciences 31, 539–554.

Ellam, R.M., Cox, K.G., 1991. An interpretation of Karoo picrite basalts in terms of interaction between asthenospheric magmas and the mantle lithosphere. Earth and Planetary Science Letters 105, 330–342.

Ellam, R.M., Carlson, R.W., Shirley, S.B., 1992. Evidence from Re–Os isotopes for plume–lithosphere mixing in Karoo flood basalt genesis. Nature 359, 718–721.

Elliot, D.H., Fleming, T.H., 2000. Weddell triple junction: the principal focus of Ferrar and Karoo magmatism during initial breakup of Gondwana. Geology 28, 539–542.

Elliot, D.H., Fleming, T.H., Kyle, P.R., Foland, K.A., 1999. Long-distance transportation of magmas in the Jurassic Ferrar Large Igneous Province, Antarctica. Earth and Planetary Science Letters 167, 89–104.

Ernst, R.E., Baragar, W.R.A., 1992. Evidence from magnetic fabric from the flow pattern of the magma in the Mackenzie giant radiating dyke swarm. Nature 356, 511–513.

Ernst, R.E., Buchan, K.L., 1997. Layered mafic intrusions: a model for their feeder systems and relationship with giant dyke swarms and mantle plume centres. South African Journal of Geology 100, 319–334.

Ferraccioli, F., Jones, P.C., Curtis, M.L., Leat, P.T., 2005a. Subglacial imprints of early Gondwana break-up as identified from high resolution aerogeophysical data over western Dronning Maud Land, East Antarctica. Terra Nova 17, 573–579.

Ferraccioli, F., Jones, P.C., Curtis, M.L., Leat, P.T., Riley, T.R., 2005b. Tectonic and magmatic patterns in the Jutulstraumen rift(?) region, East Antarctica, as imaged by high-resolution aeromagnetic data. Earth Planets Space 57, 767–780.

Ford, A.B., Himmelberg, G.R,, 1991. Geology and crystallization of the Dufek intrusion. In: Tingey, R.J. (Ed.), Geology of Antarctica. Oxford University Press, Oxford, pp. 175–214.

Foulger, G.R., 2002. Plumes, or plate tectonic processes? Astronomy and Geophysics 43, 6.19–6.23.

Grantham, G.H., 1996. Aspects of Jurassic magmatism and faulting in western Dronning Maud Land, Antarctica: implications for Gondwana break-up. In: Storey, B.C., King, E.C., Livermore, R.A. (Eds.), Weddell Sea Tectonics and Gondwana Break-up. Geological Society, London, Special Publications 108, pp. 63–73.

Grantham, G.H., Guise, P.D., Spell, T., Havenga, A., 1998. The chronology of Jurassic intrusions, H.U. Sverdrupfjella, Dronning Maud Land, Antarctica (abstract). Journal of African Earth Sciences 27 (1A), 92.

Grantham, G.H., Groenewald, P.B., Hunter, D.R., 1988. Geology of the northern H.U. Svedrupfjella, western Dronning Maud Land and implications for Gondwana reconstructions. South African Journal of Antarctic Research 18, 2–10.

Groenewald, P.M., Moyes, A.B., Grantham, G.H., Krynauw, J.R., 1995. East Antarctic crustal evolution: geological constraints and modelling in western Dronning Maud Land. Precambrian Research 75, 231–250.

Harris, C., Grantham, G.H., 1993. Geology and petrogenesis of the Straumsvola nepheline syenite complex, Dronning Maud Land, Antarctica. Geological Magazine 130, 513–532.

Harris, C., Marsh, J.S., Duncan, A.R., Erlank, A.J., 1990. The petrogenesis of the Kirwan Basalts of Dronning Maud Land, Antarctica. Journal of Petrology 31, 341–369.

Harris, C., Watters, B.R., Groenewald, P.B., 1991. Geochemistry of the Mesozoic regional basic dykes of western Dronning Maud Land, Antarctica. Contributions to Mineralogy and Petrology 107, 100–111.

Hawkesworth, C.J., Kelley, S.P., Turner, S.P., le Roex, A.P., Storey, B.C., 1999. Mantle processes during Gondwana break-up. Journal of South African Earth Sciences 28, 239–261.

Hjelle, A., 1972. Some observations on the geology of H.U. Sverdrupfjella, Dronning Maud Land. Norsk Polarinstitutt Arbok, 7–22.

Jacobs, J., Thomas, R.J., Weber, K., 1993. Accretion and indentation tectonics at the southern edge of the Kaapvaal craton during Kibaran (Grenville) orogeny. Geology 21, 203–206.

Jelínek, V., 1978. Statistical processing of anisotropy of magnetic susceptibility measured on groups of specimens. Studia Geophysica et Geodaetica 22, 50–62, doi:10.1007/BF01613632.

Jelínek, V., 1981. Characterization of the magnetic fabric of rocks. Tectonophysics 79, T63–T67, doi:10.1016/0040-1951(81)90110-4.

Jerram, D.A., Widdowson, M., 2005. The anatomy of continental flood basalt provinces: geological constraints on the processes and products of flood volcanism. Lithos 79, 385–405.

Jolly, R.J.H., 1996. Mechamism of igneous sheet intrusion. Ph.D. thesis, University of Southampton.

Jolly, R.J.H., Sanderson, D.J., 1995. The variation in the form and distribution of dykes in the Mull swarm, Scotland. Journal of Structural Geology 17, 1543–1557.

Jolly, R.J.H., Cosgrove, J.W., Dewhurst, D.N., 1998. Thickness and spatial distributions of clastic dykes, northwest Sacremento, California. Journal of Structural Geology 20, 1663–1672.

Jourdan, F., Féraud, G., Bertrand, H., Kampunzu, A.B., Tshoso, G., Le Gall, B., Tiercelin, J.J., Capiez, P., 2004. The Karoo triple junction questioned: evidence from Jurassic and Proterozoic $^{40}Ar/^{39}Ar$ ages and geochemistry of the Okavango dyke swarm (Botswana). Earth and Planetary Science Letters 222, 989–1006.

Karloukovski, V.V., 2000. Magnetostratigraphy and palaeomagnetism of the area around the Momchilgrad Palaeogene depression in the east Rhodope Massif. PhD thesis, University of East Anglia, Norwich.

Knight, M.D., Walker, G.P.L., 1988. Magma flow directions in dykes of the Koolau Complex, Oahu, determined from magnetic fabric studies. Journal of Geophysical Research 93, 4301–4319.

Koppers, A.A.P., 2002. ArArCALC – software for Ar-40/Ar-39 age calculations. Computers and Geosciences 28, 605–619.

Kyle, P.R., 1980. Development of heterogeneties in the subcontinental mantle: evidence from the Ferrar Group, Antarctica. Contributions to Mineralogy and Petrology 73, 89–104.
Le Gall, B., Tshoso, G., Dyment, J., Kampunzu, A.B., Jourdan, F., Féraud, G., Bertrand, H., Aubourg, C., Vétel, W., 2005. The Okavango giant mafic dyke swarm (NE Botswana): its structural significance within the Karoo large igneous province. Journal of Structural Geology 27, 2234–2255.
Le Gall, B., Tshoso, G., Jourdan, F., Féraud, G., Bertrand, H., Tiercelin, J.J., Kampunzu, A.B., Modisi, M.P., Dyment, J., Maia, M., 2002. 40Ar/39Ar geochronology and structural data from the giant Okavango and related mafic dyke swarms, Karoo igneous province, northern Botswana. Earth and Planetary Science Letters 202, 595–606.
Liss, D., 2003. Emplacement processes and magma flow geometries of the Whin Sill complex. PhD thesis, University of Birmingham.
Luttinen, A.V., Furnes, H., 2000. Flood basalts of Vestfjella: Jurassic magmatism across an Archaean–Proterozoic lithospheric boundary in Dronning Maud Land, Antarctica. Journal of Petrology 41, 1271–1305.
Luttinen, A.V., Rämö, O.T., Huhma, H., 1998. Nd and Sr isotopic and trace element composition of a Mesozoic CFB suite from Dronning Maud Land, Antarctica: implications for lithosphere and asthenosphere contributions to Karoo magmatism. Geochimica et Cosmochimica Acta 62, 2701–2714.
Marsh, J.S., Hooper, P.R., Rehacek, J., Duncan, R.A., Duncan, A.R., 1997. Stratigraphy and age of Karoo basalts of Lesotho and implications for correlations with the Karoo igneous province. In: Mahoney, J.J., Coffin, M.F. (Eds.), Large Igneous Provinces: Continental, Oceanic, and Planetary Flood Volcanism. Geophysical Monograph, 100. American Geophysical Union.
Moyes, A.B., Krynauw, J.R., Barton, J.M., 1995. The age of the Ritscherflya Supergroup and Borgmassivet Intrusions, Dronning Maud Land, Antarctica. Antarctic Science 7, 87–97.
Owens, W.H., 1974. Mathematical model studies on factors affecting magnetic anisotropy of deformed rocks. Tectonophysics 24, 115–131.
Owens, W.H., 1994. Laboratory drilling of field-orientated block samples. Journal of Structural Geology 16, 1719–1721.
Owens, W.H., 2000. Error estimates in the measurement of anisotropic magnetic susceptibility. Geophysical Journal International 142, 516–526.
Park, J.K., Tanczyk, E., Desbarats, A., 1988. Magnetic fabric and its significance in the 1400 Ma Mealy diabase dikes of Labrador, Canada. Journal of Geophysical Research 93, 13,689–13,704.
Pickering, G., Bull, J.M., Sanderson, D.J., 1995. Sampling power-law distributions. Tectonophysics 248, 1–20.
Rapalini, A.E., de Luchi, M.L., 2000. Paleomagnetism and magnetic fabric of Middle Jurassic dykes from Western Patagonia, Argentina. Physics of the Earth and Planetary Interiors 120, 11–27.
Raposo, M.I.B., D'Agrella-Filho, M.S., 2000. Magnetic fabrics of dike swarms from SE Bahia State, Brazil: their significance and implications for Mesoproterozoic basic magmatism in the Sao Francisco Craton. Precambrian Research 99, 309–325.
Renne, P.R., Swisher, C.C., Deino, A.L., Karner, D.B., Owens, T.L., DePaolo, D.J., 1998. Intercalibration of standards, absolute ages and uncertainties in Ar–Ar dating. Chemical Geology 145, 117–152.
Rubin, A.M., 1993. On the thermal inability of dykes leaving magma chambers. Geophysical Research Letters 20, 257–260.
Riley, T.R., Knight, K.B., 2001. Age of pre-break-up Gondwana magmatism: a review. Antarctic Science 13, 99–110.
Riley, T.R., Leat, P.T., Curtis, M.L., Millar, L.L., Fazel, A., 2005. Early-Middle Jurassic dolerite dykes from western Dronning Maud Land (Antarctica): identifying mantle sources in the Karoo large igneous province. Journal of Petrology 46, 1489–1524.
Rochette, P., Aubourg, C., Mireille, P., 1999. Is this magnetic fabric normal? A review and case studies in volcanic formations. Tectonophysics 307, 219–234.
Rochette, P., Jackson, M., Aubourg, C., 1992. Rock magnetism and the interpretation of anisotropy of magnetic susceptibility. Reviews in Geophysics 30, 209–226.
Rochette, P., Jenatton, L., Dupuy, C., Boudier, F., Reuber, I., 1991. Diabase dyke emplacement in the Oman ophiolite: a magnetic fabric study with reference to geochemistry. In: Peters, T.J., Nicolas, A., Coleman, R.G. (Eds.), Ophiolite Genesis and Evolution of the Oceanic Lithosphere. Kluwer, Dordrecht, pp. 55–82.
Spaeth, G., 1987. Aspects of the structural evolution and magmatism in western New Schwabenland, Antarctica. In: McKenzie, G.D. (Ed.), Gondwana Six: Structure, Tectonics and Geophysics. Geophysical Monograph Series, 40. American Geophysical Union, Washington, D.C, pp. 295–307.
Stevenson, C.T.E., Owens, W.H., Hutton, D.H.W., Hood, D.N., Meighan, I., 2007a. Laccolithic, as opposed to cauldron subsidence, emplacement of the Eastern Mourne pluton: evidence from anisotropy of magnetic susceptibility. Geological Society [London] Journal 164, 99–110. doi:10.1144/0016076492006-008
Stevenson, C.T.E., Owens, W.H., Hutton, D.H.W., 2007b. Flow lobes in granite: the determination of magma fl ow direction in the Trawenagh Bay Granite, northwestern Ireland, using anisotropy of magnetic susceptibility. Geological Society of America, Bulletin 119, 1368–1386. doi:10.1130/B25970.1
Storey, B.C., 1995. The role of mantle plumes in continental breakup: case histories from Gondwanaland. Nature 377, 301–308.
Sweeney, R.J., Duncan, A.R., Erlank, A.J., 1994. Geochemistry and petrogenesis of central Lebombo basalts of the Karoo igneous province. Journal of Petrology 35, 95–125.
Tauxe, L., Gee, J.S., Staudigel, H., 1998. Flow directions in dikes from anisotropy of magnetic susceptibility data: the bootstrap way. Journal of Geophysical Research 103, 17775–17790.
Watkeys, M.K., 2002. Development of the Lebombo rifted volcanic margin of southeast Africa. In: Menzies, M.A., Klemperer, S.L., Ebinger, C.J., Baker, J. (Eds.), Volcanic Rifted Margins. Geological Society of America Special Paper 362, pp. 27–46.
White, R.S., McKenzie, D.P., 1989. Magmatism at rift margins: the generation of volcanic continental margins and flood basalts. Journal of Geophysical Research 94, 7685–7729.
Wolmarans, L.G., Kent, L.E., 1982. Geological investigations in western Dronning Maud Land, Antarctica – a synthesis. South African Journal of Antarctic Research Suppl. 2.
Zhang, X., Luttinen, A.V., Elliot, D.H., Larsson, K., Foland, K.A., 2003. Early stages of Gondwana breakup: the $^{40}Ar/^{39}Ar$ geochronology of Jurassic basaltic rocks from western Dronning Maud Land, Antarctica, and implications for the timing of magmatic and hydrothermal events. Journal of Geophysical Research 108 (B9), 2449.